^{18}F-Fluoroestradiol: Current Applications and Future Directions

Sophia R. O'Brien, MD • Christine E. Edmonds, MD • Shannon M. Lanzo, MD • Joanna K. Weeks, MD • David A. Mankoff, MD, PhD
Austin R. Pantel, MD, MSTR

Author affiliations, funding, and conflicts of interest are listed at the end of this article.
See the invited commentary by Fowler in this issue.

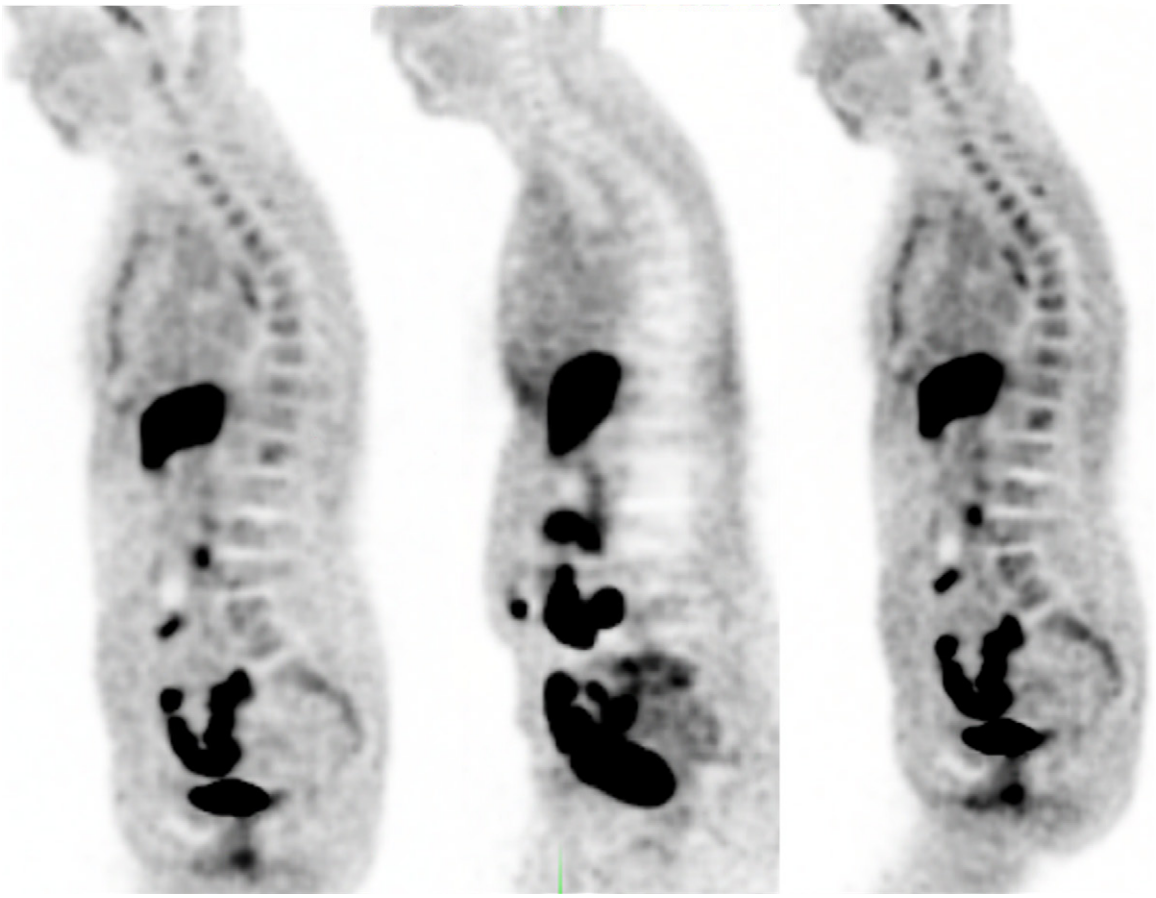

In the United States, breast cancer is the second leading cause of cancer death in all women and the leading cause of cancer death in Black women. The breast cancer receptor profile, assessed with immunohistochemical staining of tissue samples, allows prediction of outcomes and direction of patient treatment. Approximately 80% of newly diagnosed breast cancers are hormone receptor (HR) positive, which is defined as estrogen receptor (ER) and/or progesterone receptor (PR) positive. Patients with ER-positive disease can be treated with therapies targeting the ER; however, the assessment of ER expression with immunohistochemical staining of biopsy specimens has several limitations including sampling error, false-negative results, challenging or inaccessible biopsy sites, and the inability to synchronously and serially assess all metastatic sites to identify spatial and/or temporal ER heterogeneity. In May 2020, after decades of research, the U.S. Food and Drug Administration approved the PET radiotracer fluorine 18 (^{18}F) fluoroestradiol (FES) for clinical use in patients with ER-positive recurrent or metastatic breast cancer as an adjunct to biopsy. FES binds to the ER in the nucleus of ER-expressing cells, enabling whole-body in vivo assessment of ER expression. This article is focused on the approved uses of FES in the United States, including identification of a target lesion for confirmatory biopsy, in vivo assessment of biopsy-proven ER-positive disease, and evaluation of spatial and temporal ER heterogeneity. FES is an example of precision medicine that has been leveraged to optimize the care of patients with breast cancer.

Invited Commentary

Quiz questions for this article are available through the Online Learning Center.

RadioGraphics 2023; 43(3):e220143
https://doi.org/10.1148/rg.220143

Content Codes: BR, NM

Abbreviations: ER = estrogen receptor, FDA = U.S. Food and Drug Administration, ERBB2 = Erb-b2 receptor tyrosine kinase 2, FDG = fluorine 18 fluorodeoxyglucose, FES = fluorine 18 fluoroestradiol, HR = hormone receptor, MIP = maximum intensity projection, PR = progesterone receptor, SUV = standarized uptake value, SUV_{max} = maximum SUV.

TEACHING POINTS

- In the United States, FES is marketed under the trade name Cerianna (GE Healthcare) for clinical use in patients with ER-positive recurrent or metastatic breast cancer as an adjunct to biopsy.
- It is highly recommended that patients be imaged before they start ER-antagonist therapy, defined as selective estrogen receptor modulators and/or downregulators, according to current imaging indications. ER blockade with ER-antagonist therapies decreases or completely blocks FES binding to the ER, severely limiting the clinical information available for interpretation of an FES examination.
- Unlike FDG uptake, FES uptake is not seen in inflammatory, degenerative, or other reactive processes.
- A maximum standardized uptake value (SUV_{max}) of greater than or equal to 1.5 is one of the currently accepted standards for identifying FES-positive disease and is interpreted as reflecting functionally ER-positive disease. Sites of abnormal uptake can also be identified as qualitatively showing higher than local and blood pool background uptake, which is confirmed quantitatively.
- FES allows clear identification of metastasis in the lymph nodes or soft tissue, the bones, and the lungs; however, identifying liver disease is currently limited due to the high physiologic background uptake of the liver.

Introduction

Breast cancer is the most commonly diagnosed cancer in women worldwide, with one in eight women receiving the diagnosis in their lifetime (1,2). In the United States, breast cancer is the second leading cause of cancer death in all women after lung cancer and the leading cause of cancer death in Black women (3,4). The receptor profile of breast cancer allows prediction of outcomes and direction of patient treatment, and the National Comprehensive Cancer Network (NCCN) recommends receptor status testing in all patients with primary and recurrent breast cancer (5). In current practice, immunohistochemical staining of tissue biopsy specimens is the reference standard for assessment of this receptor profile. The estrogen receptor (ER), progesterone receptor (PR), and Erb-b2 receptor tyrosine kinase 2 (ERBB2; formerly HER2 [human epidermal growth factor receptor 2]) are routinely quantified (5). A breast cancer is considered hormone receptor (HR) positive if it is ER positive and/or PR positive (1).

Approximately 80% of all newly diagnosed breast cancers are HR positive. Patients with HR-positive breast cancer have the best overall prognosis. Patients with localized HR-positive disease have a 5-year survival rate of 99%–100% compared with 91%–97% for those with HR-negative localized breast cancer (1). Patients with metastatic HR-positive breast cancer have a 5-year survival rate of 32%–46% compared with 12%–40% in patients with HR-negative metastasis (1). Part of the improved survival rate is due to the use of ER-targeted therapies (also known as endocrine therapy or hormone therapy), including aromatase inhibitors (eg, anastrozole), selective ER modulators (eg, tamoxifen), and selective ER downregulators (eg, fulvestrant).

The assessment of tissue ER expression through analysis of percutaneous biopsy or surgical specimens, although essential in guiding clinical practice, has several inherent limitations. Obtaining tissue is often challenging, if not impossible, depending on the anatomic site. In addition, osseous metastases, which are common in ER-positive disease, can be difficult to sample, and cortical samples have a relatively high false-negative rate for ER positivity at immunohistochemical staining because of the decalcification procedure needed for their processing (6,7). The invasive nature of biopsy limits serial sampling and sampling of numerous sites, which precludes comprehensive assessment of disease heterogeneity. Sampling errors and laboratory differences in the analysis of the tissue present additional challenges. These limitations create the need for methods to evaluate breast cancer ER expression that are complementary to tissue assay and that provide opportunities for a noninvasive agent for imaging ER expression to improve the care of patients with ER-positive breast cancer.

In May 2020, the U.S. Food and Drug Administration (FDA) approved the PET radiotracer 16α fluorine 18 (^{18}F)-fluoro-17β estradiol or ^{18}F-fluoroestradiol (FES). FES was previously approved in France in 2016 under the trade name EstroTep for clinical use in patients with initially ER-positive breast cancer who present with recurrence or metastasis unfavorable to biopsy (8). In the United States, FES is marketed under the trade name Cerianna (GE Healthcare) for clinical use in patients with ER-positive recurrent or metastatic breast cancer as an adjunct to biopsy (9). These clinical approvals follow decades of translational and clinical studies validating this radiotracer (10).

In this article, we focus on the approved uses of FES in the United States as an adjunct to biopsy, including identification of a target lesion for confirmatory biopsy, in vivo assessment of biopsy-proven ER-positive disease including clarification of equivocal ^{18}F fluorodeoxyglucose (FDG) findings, and evaluation of spatial and temporal ER heterogeneity. In the United States, a confirmatory biopsy of FES imaging findings is strongly recommended, when possible, according to standard practices encouraging tissue confirmation of imaging or clinical findings before major changes in disease management. Beyond the current clinical applications, there are many emerging indications for FES that may become standard practice in the future, including predicting the response to systemic therapy, assessing ER blockade by ER antagonists, initial staging in patients with ER-positive disease, and imaging in other cancer populations (Table 1).

^{18}F-Fluoroestradiol

FES is an ^{18}F-labeled estradiol analog for use with PET, with anatomic correlation provided by CT as combined PET/CT imaging (Fig 1). FES binds to the ER in the nucleus of ER-expressing cells. Study results have confirmed that in vivo uptake of FES correlates with in vitro ER expression, which is assayed by both radioligand binding and immunohistochemical analysis for an accurate quantification of ER expression (11–13).

Table 1: FES Diagnostic Uses in the United States

As an adjunct to biopsy, FES can be used as follows:
Select a biopsy target
Assess the burden of ER-positive disease
Clarify FDG-avid findings
Identify spatial and/or temporal ER heterogeneity
Possible future applications:
Predict response to systemic therapy
Demonstrate effective ER blockade by an ER antagonist
Initial staging of ER-positive breast cancer
Clinical use in other patient populations

Note.—FES is currently FDA approved for detection of ER-positive lesions as an adjunct to biopsy in patients with recurrent or metastatic breast cancer.

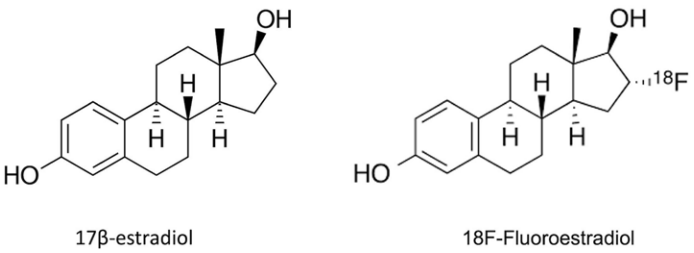

Figure 1. Illustrations show the molecular structure of 17β estradiol and of the PET radiotracer 16α fluorine 18 (^{18}F) fluoro-17β estradiol, better known as ^{18}F-fluoroestradiol (FES).

The normal distribution of FES includes the highly ER-expressing uterus and the structures involved in FES metabolism and excretion, notably the liver (the radiotracer's critical organ), biliary system, gallbladder, common bile duct, small bowel, kidneys, ureters, and bladder (Fig 2). In addition, the draining vein from the site of injection of FES is often seen containing residual radiotracer during imaging (14).

As a steroid-based compound, FES is rapidly extracted from the plasma and metabolized by the liver, with radiolabeled metabolites excreted with bile to the gallbladder and bowel. FES metabolites are efficiently resorbed by the small bowel, reenter circulation by means of the portal vein, and are then excreted by the kidneys into the urine (15). Efficient resorption from the small bowel back into the bloodstream leads to minimal to no distal large bowel uptake. The rates of metabolite release from the liver and excretion by the kidneys are similar, resulting in a relatively stable background activity for many hours after administration of FES (15,16).

Patient Preparation, Radiotracer Administration, and Imaging Protocol

FES has been used as a research agent since the 1980s and as a clinical agent since 2016 in France and 2020 in the United States, without any major adverse events reported to date (10,13,16–18).

A nuclear medicine clinical team member should verify the treatment status of the patient and the indication for FES imaging prior to the scan being scheduled, particularly while ordering physicians become familiar with this new imaging agent. It is highly recommended that patients be imaged before they start ER-antagonist therapy, defined as selective estrogen receptor modulators and/or downregulators, according to current imaging indications. ER blockade with ER-antagonist therapies decreases or completely blocks FES binding to the ER, severely limiting the clinical information available for interpretation of an FES examination. In such cases, it is impossible to determine if decreased or absent FES avidity of a lesion represents blocked ER-positive disease, treated ER-positive disease, or ER-negative disease. If patients stop ER-antagonist therapy, they may be imaged without the confounding effect of ER-blocking drugs after a washout period. However, the currently recommended washout periods (8 weeks for tamoxifen and 28 weeks for fulvestrant) are often prohibitively long, and future research is needed to clarify, and ideally shorten, these recommended washout periods (9). FES PET/CT examinations have been performed under research protocols to assess the degree of ER blockade by ER antagonists, but this is not part of routine clinical use (19,20). FES imaging may be performed in patients who are currently taking aromatase inhibitors, because these agents decrease peripheral and local estrogen production but do not block the ER. FES imaging may also be performed in patients who are currently taking cyclin-dependent kinase (CDK4 or CDK6) inhibitors, because these do not interact with the ER (21).

Patient preparation for FES imaging is relatively straightforward. Hydration should be encouraged before and after imaging, with frequent voiding to reduce bladder exposure to radiolabeled metabolites in the urine. No specific diet, fasting, or laboratory testing is necessary before the examination, except for a pregnancy test in patients with childbearing potential (9).

FES can be used in men and women and in both pre- and postmenopausal women, because physiologic estrogen levels do not affect FES uptake (16,22). There are few published studies on the application of FES PET/CT in men with breast cancer, which is a topic needing further study.

There are no known contraindications to imaging with FES; however, no dedicated studies have been performed in pregnant or lactating women or in children (9). Per the Cerianna package insert, lactating women are recommended to avoid breastfeeding for 4 hours after administration of FES, but no details are provided on the handling of milk that may be pumped during that time or on any contact limitations between child and mother (9). Studies are needed to assess the excretion of FES in breastmilk and to evaluate safety metrics for feeding such milk to infants. Paralleling recommendations given after administration of FDG, lactating mothers should likely be advised to limit close contact with their child for 12 hours after injection of FES to limit the infant's exposure to radiation from the mother's body, although this recommendation is not specifically detailed in the Cerianna package insert (9,23). In addition, the Nuclear Regulatory Commission (NRC) recommends that pumped milk of mothers who have been given most radiopharmaceuticals can generally be stored for 10 physical half-lives, enabling 99.999% radioactive decay of the radioisotope;

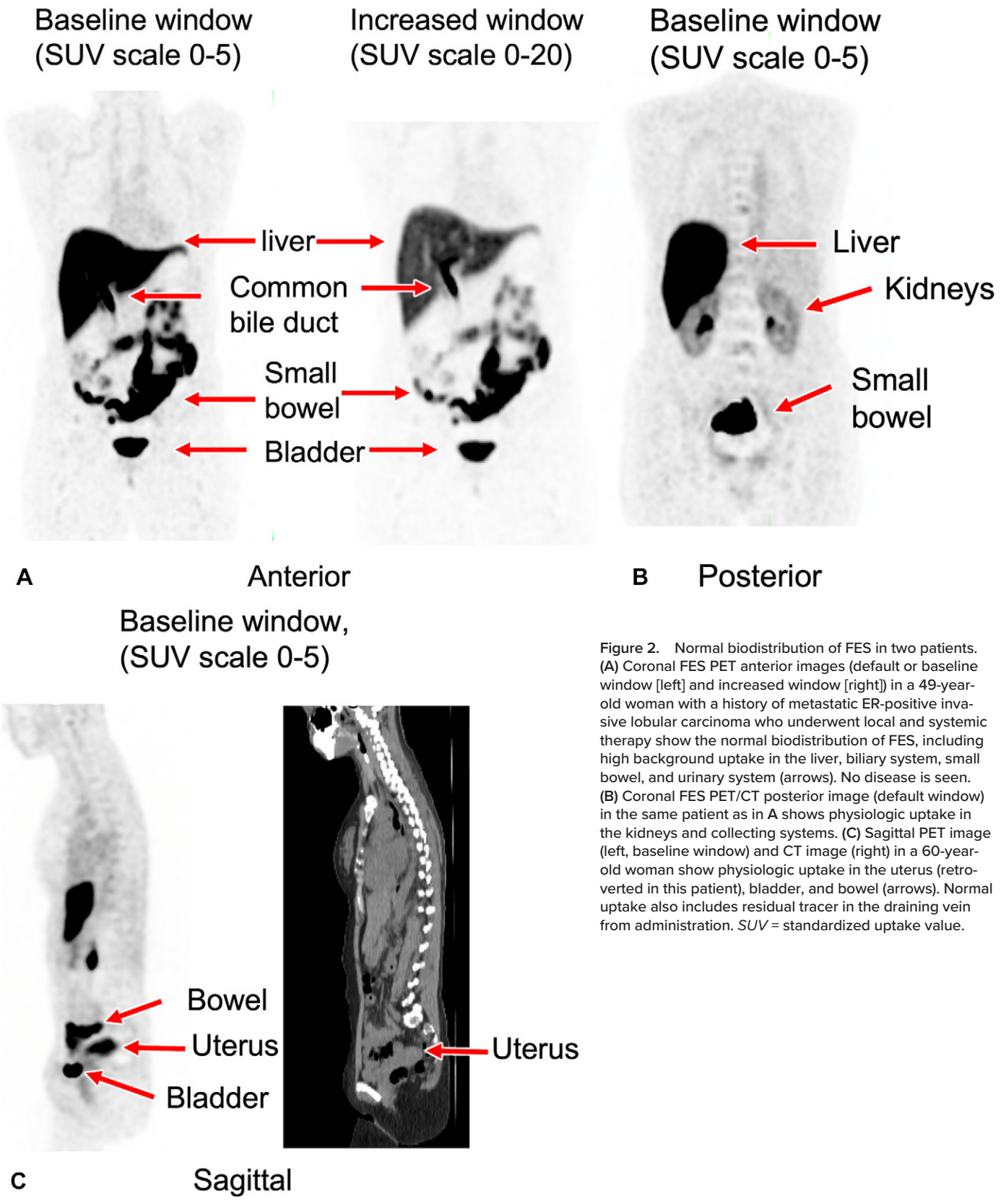

Figure 2. Normal biodistribution of FES in two patients. **(A)** Coronal FES PET anterior images (default or baseline window [left] and increased window [right]) in a 49-year-old woman with a history of metastatic ER-positive invasive lobular carcinoma who underwent local and systemic therapy show the normal biodistribution of FES, including high background uptake in the liver, biliary system, small bowel, and urinary system (arrows). No disease is seen. **(B)** Coronal FES PET/CT posterior image (default window) in the same patient as in **A** shows physiologic uptake in the kidneys and collecting systems. **(C)** Sagittal PET image (left, baseline window) and CT image (right) in a 60-year-old woman show physiologic uptake in the uterus (retroverted in this patient), bladder, and bowel (arrows). Normal uptake also includes residual tracer in the draining vein from administration. *SUV* = standardized uptake value.

however, more work is needed to quantify the levels of FES excretion in breast milk and to determine if the mass levels are low enough to ensure the safety of the milk after radioactive decay (24).

The recommended dose of FES is 6 mCi (222 MBq), with an acceptable range of 3–6 mCi (111–222 MBq). FES is administered, preferably with a syringe pump, as a 1–2-minute intravenous infusion followed by an intravenous flush of at

least 10 mL of normal saline solution. Patients are encouraged to void immediately before imaging to reduce activity in the bladder, which could obscure adjacent disease.

Imaging is optimally performed 60–80 minutes after injection of the radiotracer. Some investigators (15) have suggested that FES may be performed as early as 20 minutes after injection to avoid confounding bowel tracer in the abdomen, but this timing may not be optimal for evaluating tumor binding and requires more study (15). Patients are imaged in the supine position on the PET/CT scanner, with their arms above their head, and images are obtained from the vertex or skull base to the midthigh.

Imaging Interpretation

The normal organs to which FES is biodistributed are the uterus, liver, biliary system, gallbladder, common bile duct, small bowel, kidneys, ureters, and bladder (Fig 2). The draining vein from the site of FES injection often demonstrates residual radiotracer avidity. Confirmation of uterine uptake in patients with a uterus can serve as an internal control, demonstrating adequate FES tissue targeting and uptake (25).

FES uptake is specific for functional ER expression. A 2020 meta-analysis (26) showed specificity for ER-positive breast cancer of 98%. This specificity is more definitive in the interpretation of FES avidity: Sites of FES uptake outside the normal biodistribution are considered FES positive (commonly referred to as FES-positive disease), except for a few instances of false-positive results. Meta-analyses (27, 28) have demonstrated slightly lower sensitivity of 71%–82%; however, a 2022 prospective study (29) with 200 patients demonstrated sensitivity of 95%. Unlike FDG uptake, FES uptake is not seen in inflammatory, degenerative, or other reactive processes. Therefore, readers can expect to see no FES uptake in sites of FDG uptake related to inflammation without a tumor present, and they can expect FES uptake to resolve in sites of fully treated disease with minimal or nonviable tumor left as long as there are no confounding blocking agents (eg, tamoxifen and fulvestrant) (Fig 3). An exception is in patients with radiation pneumonitis, who can demonstrate increased FES activity that is likely related to physiologic uptake seen in lung atelectasis and/or extravasation of contrast material via leaky vessels.

A maximum standardized uptake value (SUV_{max}) of greater than or equal to 1.5 is one of the currently accepted standards for identifying FES-positive disease and is interpreted as reflecting functionally ER-positive disease. Sites of abnormal uptake can also be identified as qualitatively showing higher than local and blood pool background uptake, which is confirmed quantitatively. Because the average SUV of FES-positive disease is generally lower than that seen with other radiotracers, readers must remember to adjust windows appropriately when interpreting FES PET images. In evaluation for sites of primary disease or metastasis, the SUV upper window should be set at 2.5–5, and typically toward the lower end of this range. This window setting allows better identification of disease, but it makes sites of normal physiologic uptake (eg, the liver) or activity (eg, the bowel or bladder) hyperintense. Readers must remember to adjust the window to a higher upper SUV for evaluation within and around these high–background uptake structures to ensure that intense physiologic uptake does not obscure nearby disease (Fig 2A, 2B).

Clinical Indications for FES PET/CT in Patients with Breast Cancer

FES is approved for use in the United States as an adjunct to biopsy in patients with ER-positive recurrent or metastatic breast cancer. Under this indication, FES informs selection of a biopsy target to stage disease (Fig 4). FES can also be used for in vivo assessment of the ER-positive disease burden, including clarification of FDG imaging findings and determination of spatial and/or temporal ER heterogeneity through confirmatory biopsy. The most common sites for breast cancer to metastasize are the lymph nodes, bones, lungs, and liver (30). FES allows clear identification of metastasis in the lymph nodes or soft tissue, the bones, and the lungs; however, identifying liver disease is currently limited due to the high physiologic background uptake of the liver.

Because reactive or inflammatory processes are not FES avid, abnormal FES uptake is clear evidence of ER-positive osseous and nodal metastases (Figs 5, 6). In fact, anecdotally, we noted that FES sometimes allows visualization of more osseous metastases than does technetium 99m (^{99m}Tc) methylene diphosphonate bone scintigraphy (Fig 7), although dedicated research comparing the two imaging studies has not been performed, to our knowledge. FES can clearly show metastases to the lungs, which are another common site of metastasis (Fig 8), and pleural disease (Fig 9). FES uptake can be seen in patients with pulmonary atelectasis and radiation pneumonitis and related fibrosis, but in most cases, these conditions can be distinguished from metastasis on the basis of correlative anatomic findings on CT images (31). Because there is no background uptake in the brain, FES can also allow clear identification of brain metastases, but it should not be used as a screening modality for brain metastases.

FES can also help to clarify indeterminate FDG-avid findings in patients with recurrent or metastatic ER-positive breast cancer, with confirmatory biopsy recommended. Equivocal FDG uptake can be confirmed to represent FES-avid sites of ER-positive disease on a positive FES scan. Equivocal uptake seen on FDG PET/CT images without corresponding FES uptake may be interpreted as reactive or inflammatory, but such discordant lesions may also represent sites of FES-negative metastasis. FES-negative sites of disease are sites of primary or metastatic breast cancer with FES uptake that is qualitatively equal to or less than that of the blood pool and quantitatively with an SUV_{max} of less than 1.5. If FES-negative disease cannot be ruled out on the basis of imaging characteristics or the patient's clinical context, biopsy or close surveillance should be pursued. Biopsy of such lesions can be particularly informative if it helps to confirm a site of ER-negative metastasis, which usually prompts a change to treatment other than endocrine therapy.

FES specificity for ER-positive disease can help to clarify equivocal FDG uptake seen in axillary lymph nodes (Fig 10), internal mammary lymph nodes (Figs 11, 12), and in the surgical bed (Fig 13). Obtaining tissue can be challenging, if not

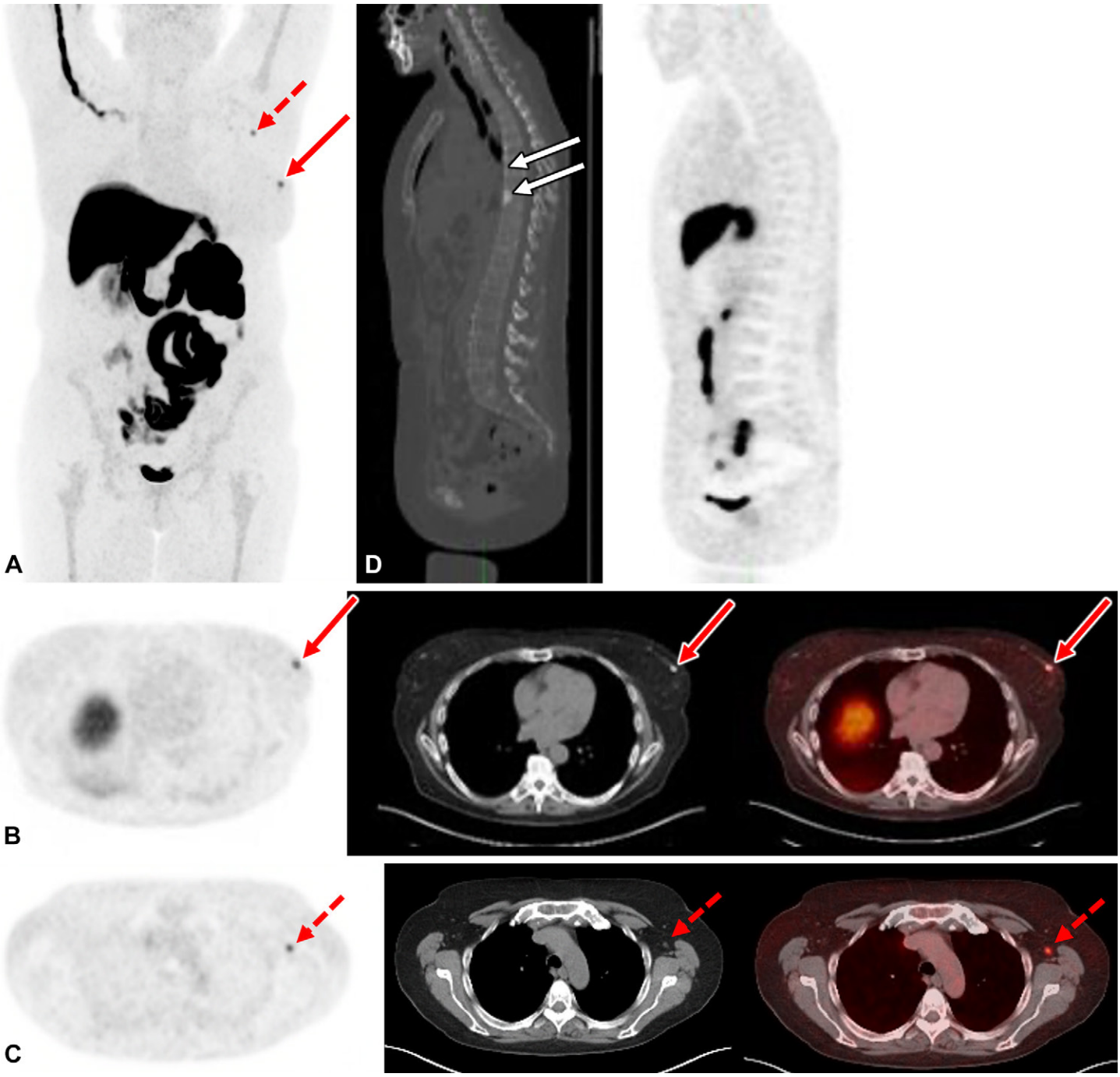

Figure 3. Metastatic estrogen receptor (ER)–positive, progesterone receptor (PR)–positive, Erb-b2 receptor tyrosine kinase 2 (ERBB2)–negative (formerly HER2 [human epidermal growth factor receptor 2]) bilateral invasive moderately differentiated ductal carcinoma, with osseous involvement, in a 60-year-old woman who underwent multiple rounds of chemotherapy, ER-targeted therapy, and radiation therapy and presented with biopsy-proven left-sided poorly differentiated invasive ductal carcinoma with micropapillary features. **(A)** Coronal maximum intensity projection (MIP) FES PET image shows abnormal FES uptake in the left breast (solid arrow) and the left axilla (dashed arrow); expected uptake in the draining vein from administration of FES in the right upper extremity; and normal uptake in the liver, bowel, and bladder. **(B)** Axial FES PET (left), CT (middle), and fused PET/CT (right) images show abnormal FES uptake (maximum SUV [SUV_{max}], 3.3) in the left breast (arrows) that suggests an ER-positive recurrence adjacent to a biopsy clip. **(C)** Axial FES PET (left), CT (middle), and fused PET/CT (right) images show abnormal FES uptake in a small left axillary lymph node (dashed arrows), measuring 8 mm × 5 mm (SUV_{max}, 3.1), which appears to be ER-positive nodal metastasis. **(D)** Sagittal CT image (left) shows scattered sclerotic vertebral lesions (arrows) that are not FES avid on the FES PET image (right), which are findings typical of treated disease. Additional cross-sectional imaging 6 months after this examination (not shown) showed stable sclerotic osseous metastases.

impossible, depending on the anatomic site. Osseous metastasis, which is common in patients with ER-positive disease, can be difficult to sample, and cortical samples demonstrate a relatively high false-negative rate for ER positivity at immunohistochemical analysis due to the decalcification procedure used in sample processing (6,7). Marrow uptake on an FES scan clarifies that the uptake seen on FDG images is, in fact, malignant instead of reactive (Figs 14, 15) and allows characterization of focal FDG-avid osseous lesions as either degenerative or metastatic ER-positive disease (Fig 16).

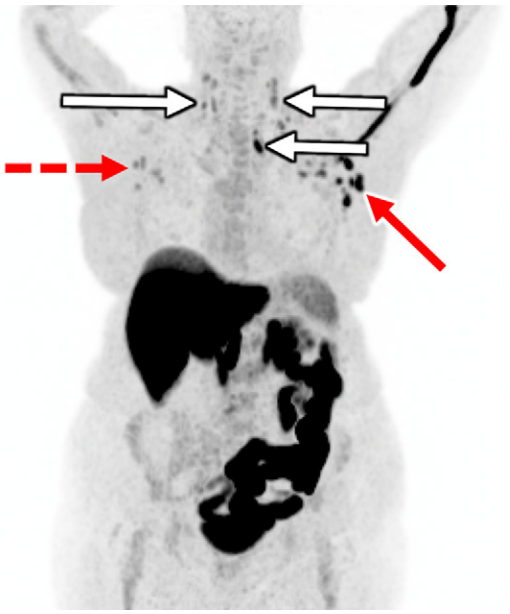

Figure 4. Grade 2 ER-positive, PR-positive, ERBB2-negative invasive lobular carcinoma of the left breast in a 76-year-old woman with indeterminate right axillary lymph nodes seen on staging FDG PET/CT images (not shown). Coronal MIP FES PET image shows uptake in known metastatic left axillary lymph nodes (SUV_{max}, 9.6, solid red arrow) and FES-avid right axillary (SUV_{max}, 3.0; dashed red arrow) and bilateral cervical and left supraclavicular (SUV_{max}, 3.5; white arrows) lymph nodes suspicious for metastasis. Biopsy of a right axillary and right cervical lymph node confirmed ER-positive metastasis at both sites. The patient's cancer was upstaged to stage 4, substantially affecting her treatment plan. Normal FES uptake is also seen in the liver, bowel, and draining vein from administration of FES in the left upper extremity (SUV scale, 0–5).

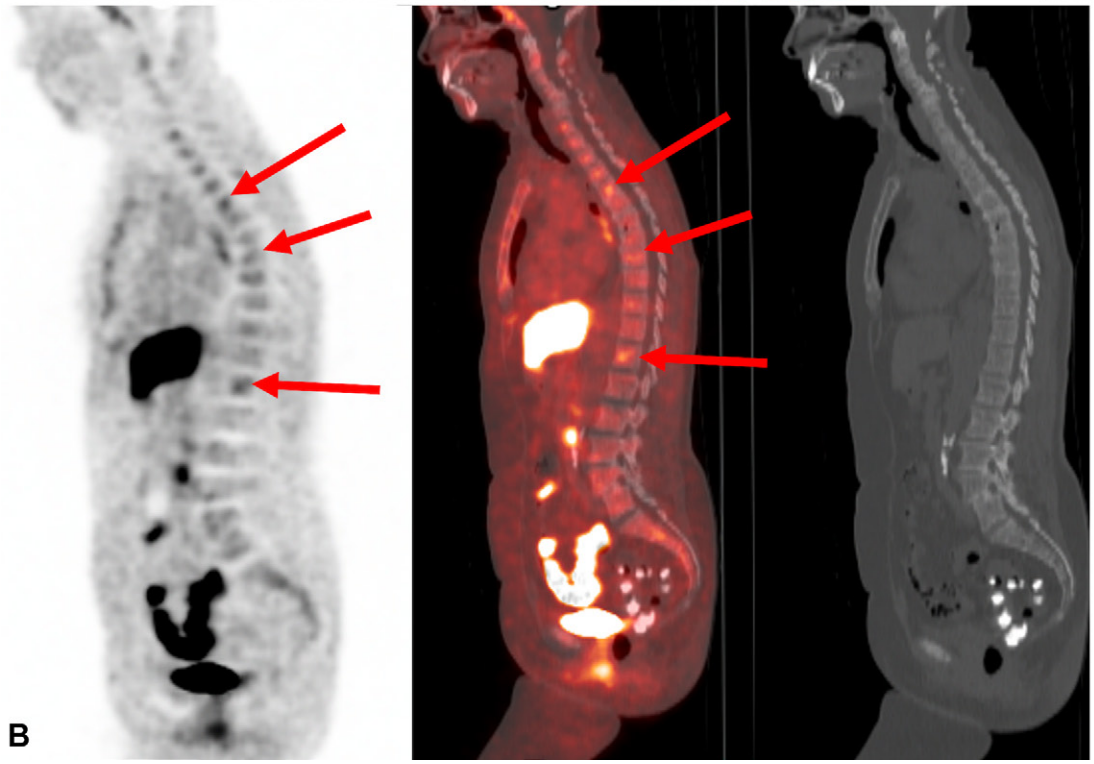

Figure 5. ER-positive invasive lobular carcinoma in a 66-year-old woman with biopsy-proven ER-positive left supraclavicular nodal metastasis and presumed ER-positive osseous metastases. **(A)** Coronal FES PET (left) and coronal fused FES PET/CT (middle) images show abnormal FES uptake in the left supraclavicular nodes (arrows) suggestive of functionally ER-positive metastasis. Coronal CT image (right) shows anatomic correlation. **(B)** Sagittal FES PET (left) and sagittal fused FES PET/CT (middle) images show abnormal FES uptake in multiple vertebrae (arrows). Sagittal CT image (right) shows no corresponding anatomic abnormality; however, this does not decrease the level of suspicion based on the abnormal FES uptake (SUV scale, 0–5).

Figure 6. ER-positive, PR-positive, ERBB2-negative breast cancer with mixed ductal and lobular features in a 68-year-old woman. The SUV scale was 0–5 in all PET images. **(A)** Axial FES PET image through the pelvis (left) and fused FES PET/CT image (middle) show abnormal FES uptake in the left ilium (arrows), and axial CT image (right) shows a corresponding sclerotic abnormality. Biopsy of this site revealed ER-positive metastasis. Normal physiologic activity in the small bowel is also seen on the FES PET and fused PET/CT images (left and middle). **(B)** Sagittal FES PET (left) and sagittal fused PET/CT (middle) images show abnormal FES uptake in the T4 vertebral body (dashed arrows), and sagittal CT image (right) shows a corresponding new sclerotic lesion, which was presumed to represent ER-positive metastasis. Normal high background FES uptake is seen in the liver on the sagittal FES PET (left) and fused FES PET/CT (middle) images.

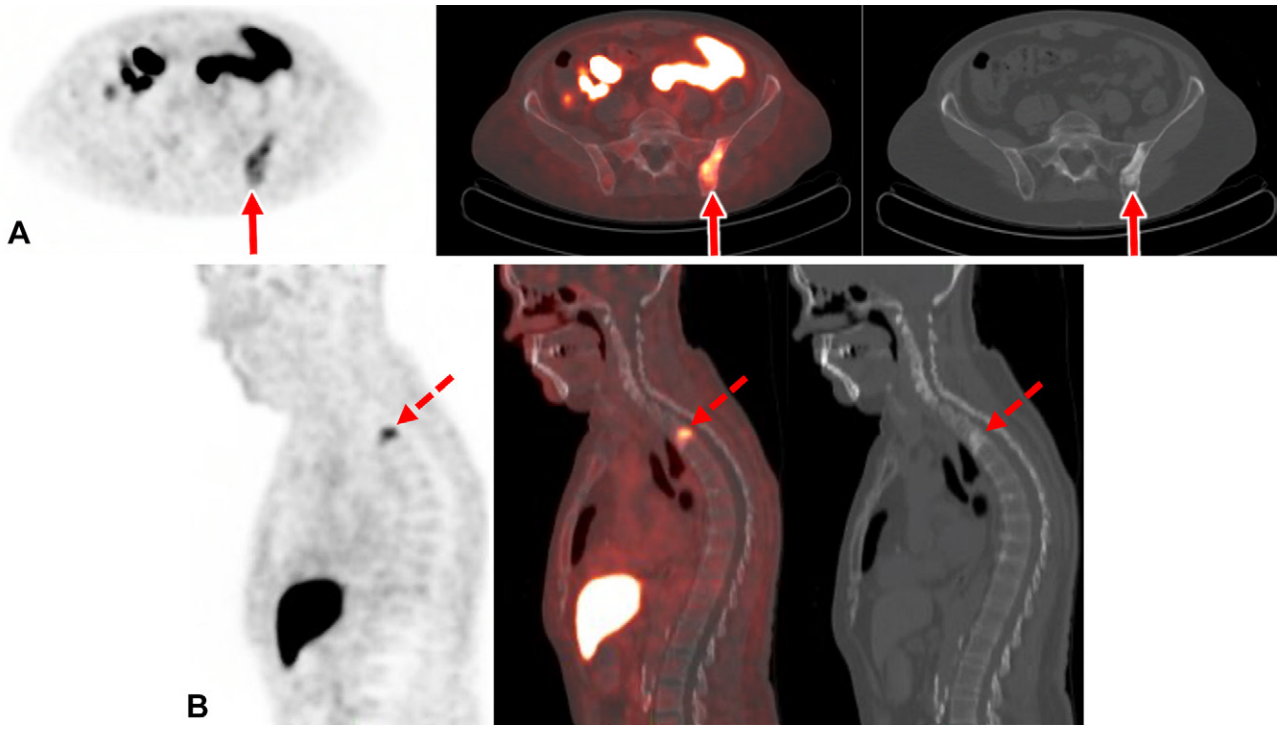

Heterogeneous ER disease (ie, with both ER-positive and ER-negative sites) represents a clinical dilemma and a patient population with outcomes worse than those for patients with homogeneous ER-positive disease (32,33). Studies have demonstrated spatial heterogeneity, with discordant ER status between the primary breast cancer and distant metastatic sites, in 15%–45% of patients with metastatic breast cancer (34–36). Temporal heterogeneity of ER expression has also been observed, with 8%–33% of patients demonstrating discordance of ER and PR expression at their primary tumor site at core-needle biopsy and at the same site after neoadjuvant chemotherapy (37). It is not practical to perform tissue biopsy of all sites of metastasis to determine ER status or to perform serial sampling of primary and metastatic sites to evaluate ER status over the course of treatment. However, FES can be used to evaluate the regional heterogeneity of ER expression of primary and metastatic breast cancer noninvasively at a single time point and temporal heterogeneity at serial imaging (38,39). The absence of FES uptake in a lesion identified with other imaging modalities, especially with FDG PET/CT, can help direct a biopsy that allows identification of ER-negative disease, which, if confirmed at immunohistochemical analysis, is likely to change patient treatment.

Limitations of FES PET/CT

Perhaps the most substantial limitation of FES PET/CT at the time of publication is the inability to evaluate liver lesions accurately, especially given that the liver is a common site of breast cancer metastasis (30). The high physiologic background uptake of the liver secondary to radiotracer metabolism can obscure ER-positive disease (Fig 17). Even large liver metastases visible on FES PET/CT images may demonstrate less uptake than that of the hepatic background parenchyma (Fig 18). Hepatic lesions with decreased FES uptake relative to the liver, even with a lesional SUV_{max} higher than 1.5, are difficult to interpret. These lesions may be further interrogated with MRI, and biopsy may be necessary for definitive characterization. Optimizing the evaluation of the liver with FES is a topic of ongoing research (40).

Similar to all imaging tests, FES PET/CT can produce false-positive and false-negative results. False-positive results include benign ER-positive nonbreast entities such as uterine fibroids, and, less commonly, meningiomas (41,42). There can be modest ER expression in the normal lung, and an atelectatic lung may show increased uptake higher than that of the background (31). Similarly, radiation pneumonitis has also been shown to be FES positive (Fig 19) (43). Physiologic FES uptake can be seen in normal and atelectatic lungs, and a similar process may explain the FES uptake in radiation pneumonitis. Extravasation of tracer via leaky vessels after radiation therapy may be another cause of FES uptake.

False-negative results at FES PET/CT include small lesions, those with low ER expression, and those adjacent to or within areas of high-FES background uptake such as hepatic lesions, peritoneal metastases close to bowel, and bowel metastases (Fig 20). The normal endometrium has high ER expression

Figure 7. Recurrent metastatic ER-positive poorly differentiated ductal carcinoma in a 70-year-old woman. **(A)** ^{99m}Tc-methylene diphosphonate whole-body anterior (left) and posterior (right) bone scintigrams reveal widespread osseous metastases. **(B)** Sagittal FES PET (left), CT (middle), and FES fused PET/CT (right) images show a far greater extent of metastasis, involving all visualized osseous structures (SUV scale, 0–5). This patient had biopsy-proven ER-positive liver metastases and presumed osseous metastases on images from multiple imaging modalities, which showed treatment response to systemic therapy on subsequent FDG PET/CT images (not shown).

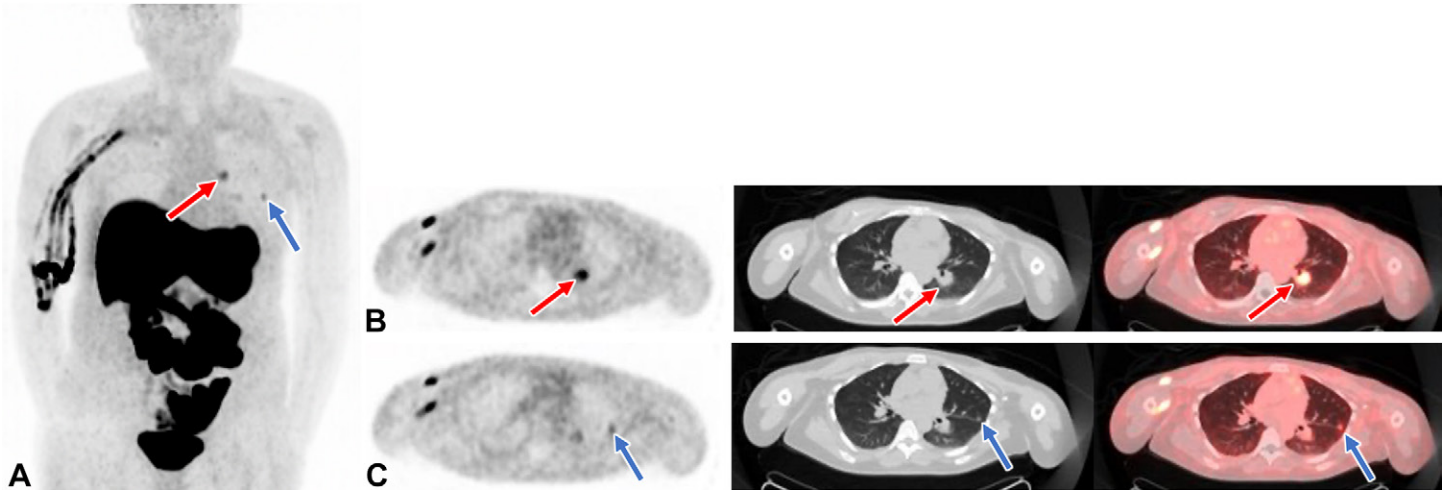

Figure 8. Metastatic ER-positive invasive ductal carcinoma in a 43-year-old woman. She subsequently presented with biopsy-proven ER-positive liver metastases and presumed lung and hilar lymph node metastases seen on chest CT and FDG PET/CT images (not shown). **(A)** Coronal MIP FES PET image shows abnormal uptake in the left hilum (red arrow) and the left pulmonary nodule (blue arrow). Normal FES uptake is seen in the liver, bowel, and bladder. **(B)** Axial FES PET (left), anatomic CT (middle), and fused FES PET/CT (right) images show FES uptake in the left hilum (arrows; SUV_{max}, 3.5), which suggests nodal metastasis. **(C)** Axial FES PET (left), anatomic CT (middle), and fused FES PET/CT (right) images show uptake in the left pulmonary nodule (arrows; SUV_{max}, 1.5), which was presumed to be metastatic. Note that the biopsy-proven liver metastases are not seen on the FES PET/CT images (SUV scale, 0–2.5).

and demonstrates FES uptake in both pre- and postmenopausal patients. Thus, the spread of ER-positive breast cancer, particularly lobular cancer, is difficult to discern from normal uterine uptake. However, the spread of FES-positive metastases to other areas of the abdomen and pelvis that are visualized with FES PET/CT can raise concern for a uterine finding that may be identified with other imaging methods, allowing differentiation from normal uterine uptake. The ovaries do not demonstrate substantial FES uptake and are often poorly visualized on FES PET/CT images (14).

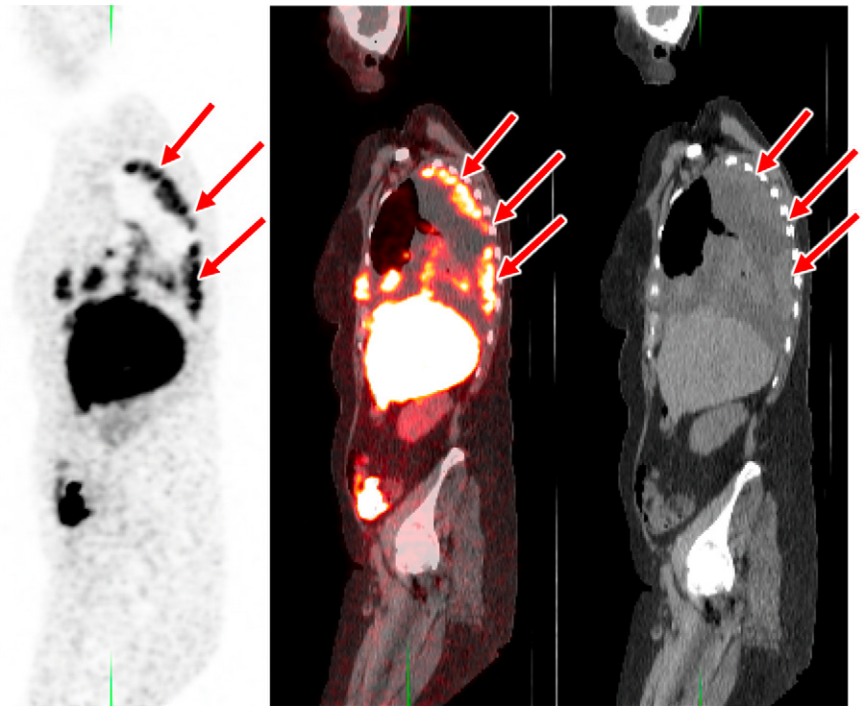

Figure 9. Metastatic ER-positive invasive ductal carcinoma in a 60-year-old woman who underwent mastectomy in 1993 and presented with increased chest discomfort and difficulty breathing in 2019. Sagittal FES PET (left) and fused FES PET/CT (middle) images show FES uptake in right pleural-based metastases (arrows), and sagittal CT image (right) shows a large likely malignant right pleural effusion (SUV scale, 0–5). Subsequent biopsy results of a right lung mass showed ER-positive recurrence. The patient was imaged under a research protocol.

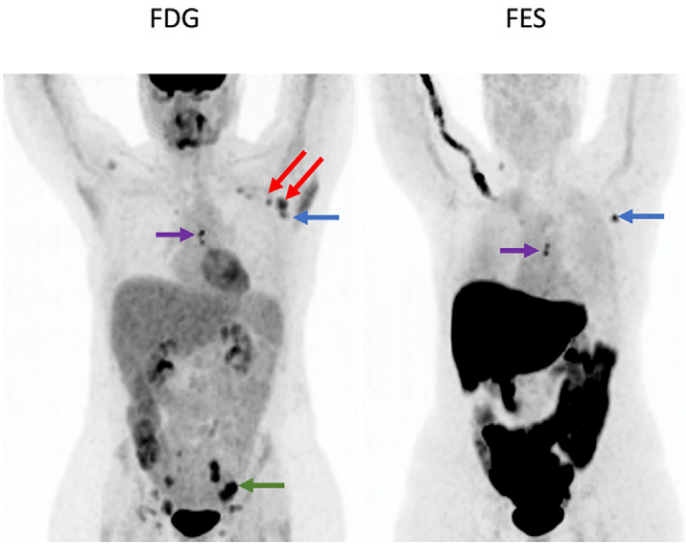

Figure 10. Metastatic ER-positive invasive ductal carcinoma and equivocal FDG-avid findings in a 44-year-old woman. Coronal MIP FDG PET image (left) shows abnormal FDG uptake in the left axillary lymph nodes (red and blue arrows, left), the internal mammary lymph nodes (purple arrow, left), and the pelvic nodes (green arrow). Coronal MIP FES PET image (right) shows abnormal FES uptake in a single left axillary lymph node (blue arrow, right), which showed ER-positive metastasis at biopsy, and in the internal mammary lymph nodes (purple arrow, right), which is consistent with ER-positive disease, but no abnormal FES uptake in the high axillary lymph nodes or the pelvic nodes. One of the high axillary lymph nodes (red arrows, left) showed reactive changes at biopsy. Because reactive or inflammatory changes are not FES avid, abnormal FES uptake in lymph nodes is highly specific for FES-positive, functionally ER-positive metastasis. Thus, FES PET allows clarification of indeterminate FDG findings (SUV scale, 0–5).

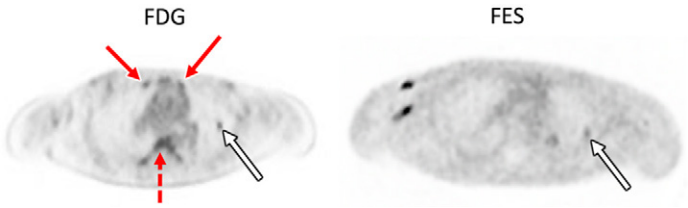

Figure 11. Metastatic ER-positive invasive ductal carcinoma in a 43-year-old woman who underwent bilateral mastectomy, with implantation of bilateral tissue expanders. Axial restaging FDG PET image (left) shows indeterminate bilateral internal mammary lymph nodes (solid red arrows), diffuse bone marrow uptake (dashed red arrow), and FDG-avid pulmonary metastasis (white arrow, left). Axial FES PET image (right) shows no abnormal FES uptake in the internal mammary nodes or bone marrow, suggesting reactive changes with false-positive FDG uptake on the FDG PET image. Although biopsy was not pursued, clinical and imaging follow-up for many years showed no metastasis in the internal mammary nodes or vertebrae. The FDG-avid pulmonary nodule did show abnormal FES uptake (white arrow, right) (SUV_{max}, 1.5), suggestive of ER-positive metastasis, which, although biopsy was not performed, did respond to ER-targeted therapy, consistent with ER-positive disease (SUV scale, 0–5).

Potential Future Uses of FES

Investigators of many ongoing research studies are evaluating additional uses of FES in patients with breast cancer and other patient populations (44). Potential future uses include initial staging of invasive lobular carcinoma, which can be occult or understaged with conventional breast imaging (45). Results of small studies have demonstrated that FES can be used to problem solve equivocal conventional staging of invasive lobular carcinoma and that FES allows identification of more sites of invasive lobular carcinoma metastases than does FDG (46,47). Low-grade invasive ductal carcinoma may also benefit from staging with FES PET/CT. Early studies (46,47) suggested that FES can be helpful in staging low-grade ER-positive breast cancer (especially lobular cancer), adding value to CT, bone scintigraphy, and FDG PET/CT, but more studies are needed. Authors of multiple clinical trials are currently investigating the use of FES for initial staging in patients with locally advanced ER-positive breast cancer.

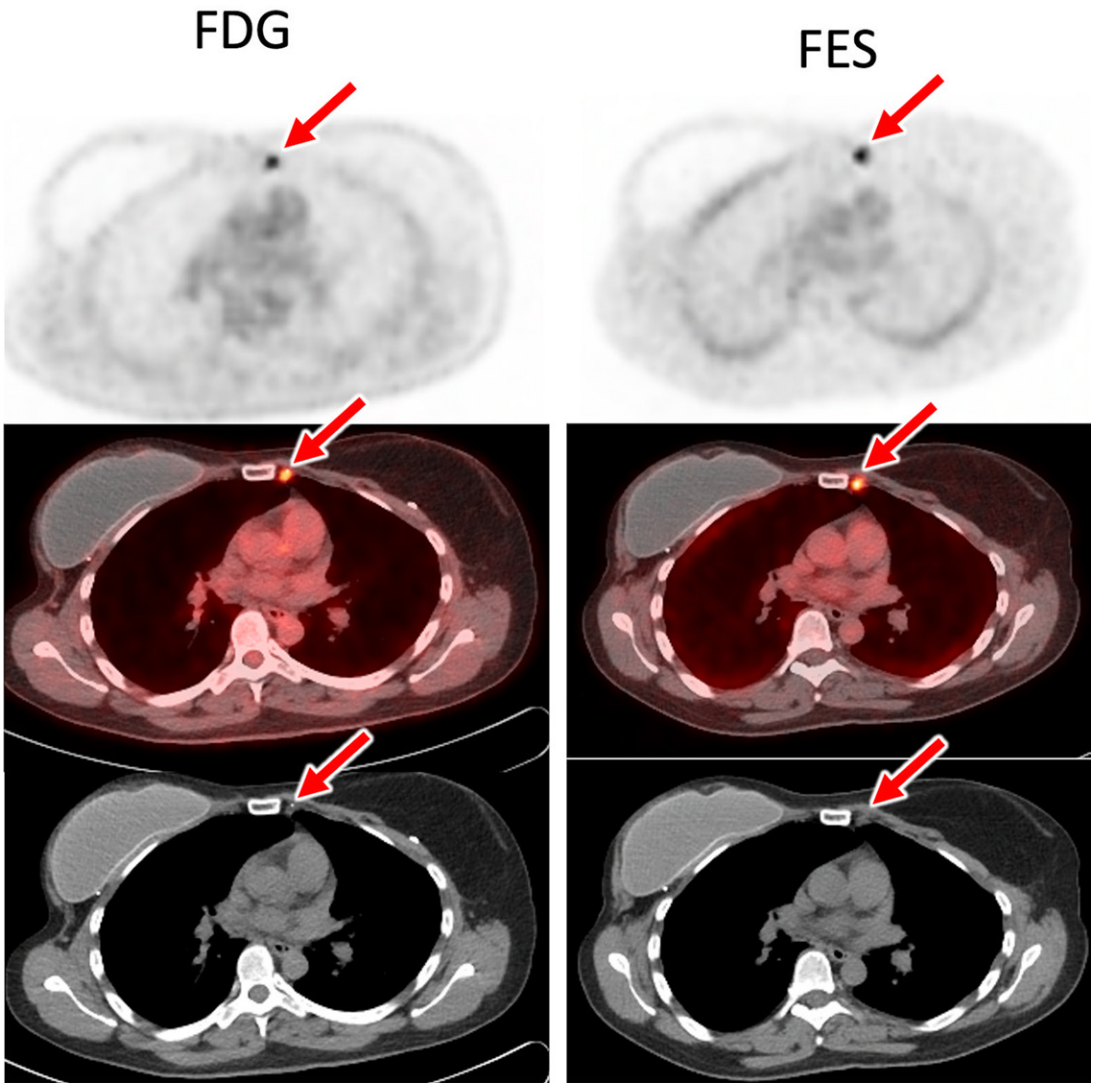

Figure 12. ER-positive invasive ductal carcinoma of the right breast, with lymphovascular invasion seen at mastectomy, with minimal response to neoadjuvant chemotherapy, radiation therapy, and ER-targeted therapy, in a 44-year-old woman currently presenting with a biopsy-proven ER-positive axillary recurrence in the left axilla. An enlarged left internal mammary node was seen at breast MRI (not shown). Axial FDG PET (top left), fused FDG PET/CT (middle left), and axial CT (bottom left) images show abnormal uptake in a left internal mammary lymph node (arrows). Axial FES PET (top right), fused FES PET/CT (middle right), and axial CT (bottom right) images show concordant abnormal FES uptake (arrows) in the left internal mammary lymph node, which suggests FES-positive, functionally ER-positive metastasis (SUV scale, 0–5 for all images).

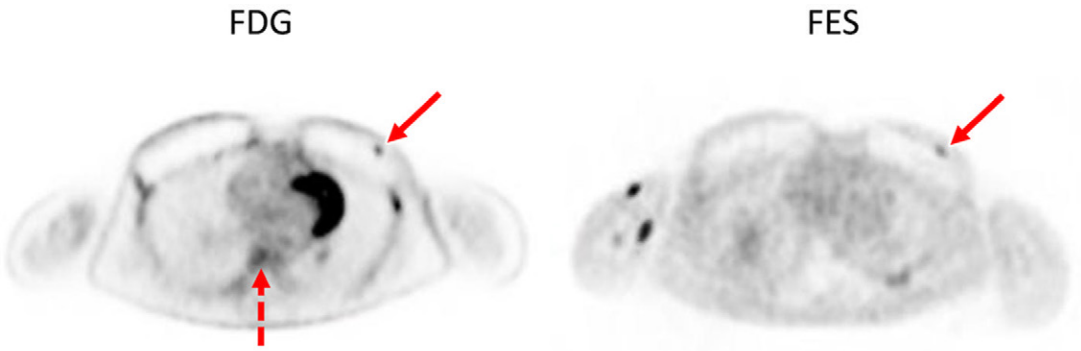

Figure 13. Metastatic ER-positive invasive ductal carcinoma after bilateral mastectomy and placement of tissue expanders in a 43-year-old woman. Axial restaging FDG PET image (left) shows peripheral FDG avidity and a focus of indeterminate FDG avidity anterior to the left tissue expander (solid arrow, left) and diffuse bone marrow uptake (dashed arrow, left). Axial FES PET image shows no FES activity around the tissue expanders, confirming that the FDG avidity is postsurgical change (SUV scale, 0–5) rather than residual disease. No FES uptake appears in the bone marrow, clarifying reactive FDG avidity, which is consistent with the lack of progressive marrow or bone findings on subsequent imaging studies (not shown). A concordant focus of FES uptake anterior to the left tissue expander is presumed to be residual functionally ER-positive disease (SUV_{max} 2.0; arrow, right). The FES avidity in the left upper extremity is expected activity in the draining vein from FES administration. This patient also had concordant FDG- and FES-positive pulmonary, nodal, and sternal metastases (not shown) and underwent systemic therapy without additional biopsies or resection (SUV scale, 0–5).

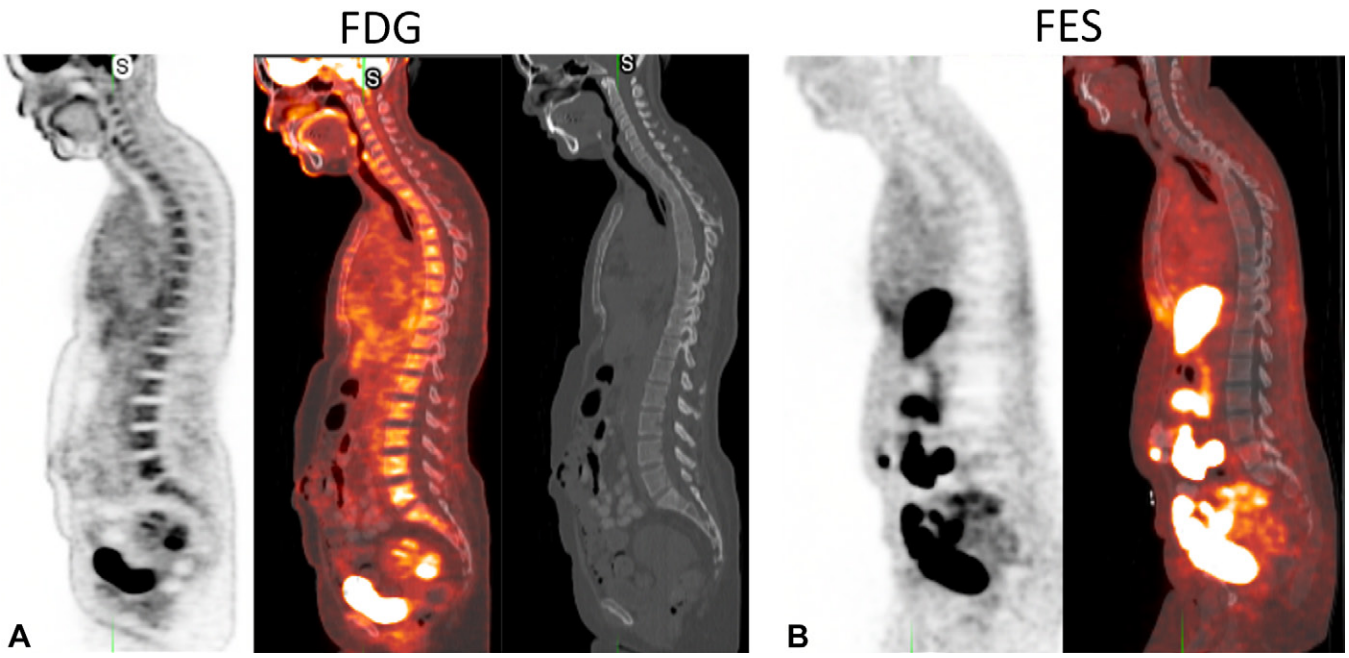

Figure 14. Metastatic ER-positive invasive ductal carcinoma in a 43-year-old woman. **(A)** Sagittal FDG PET (left) and fused FDG PET/CT (middle) images show uptake throughout the bone marrow, although the corresponding sagittal anatomic CT image (right) did not demonstrate vertebral abnormalities. This distribution of FDG uptake is indeterminate and could reflect widespread marrow disease or reactive marrow (SUV scale, 0–3.5). **(B)** Sagittal FES PET (left) and fused FES PET/CT (right) images show no FES uptake in the bone marrow, clarifying that the FDG findings represented reactive marrow (SUV scale, 0–5). The patient did not show osseous metastasis in multiple years of imaging follow-up.

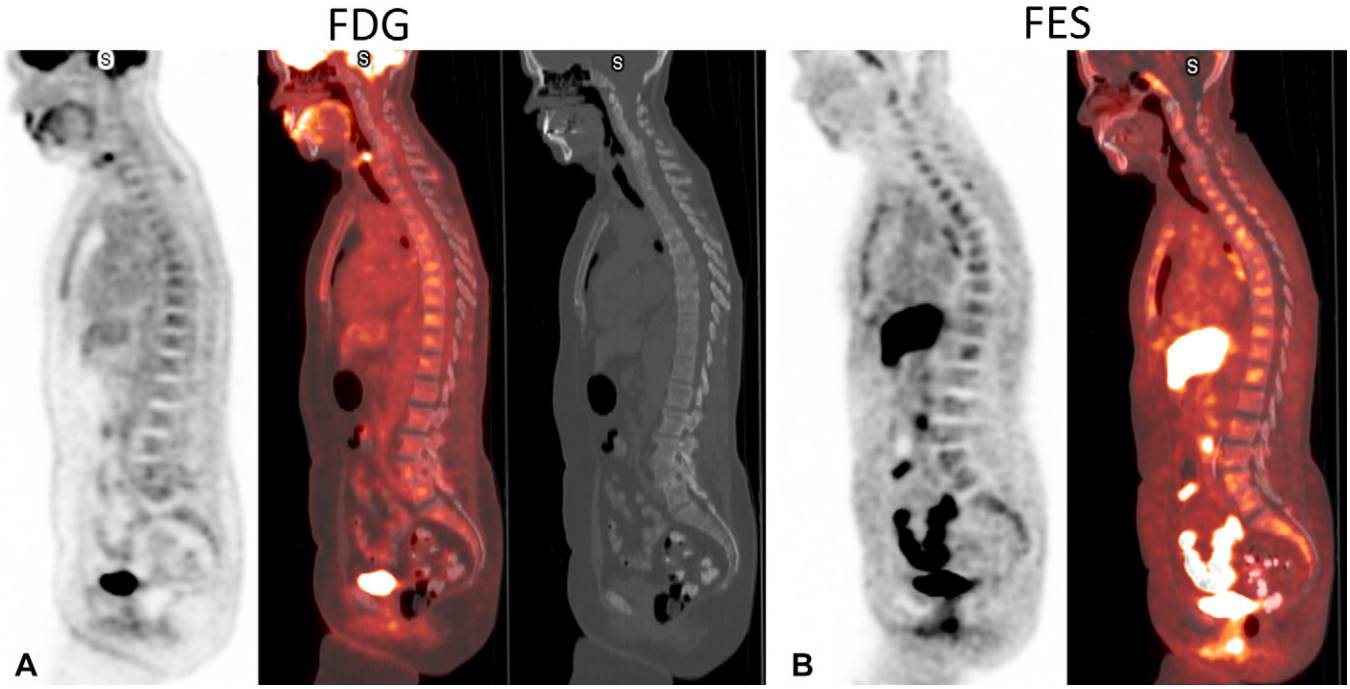

Figure 15. Metastatic ER-positive invasive lobular carcinoma with biopsy-proven ER-positive nodal metastasis and presumed ER-positive osseous metastases in a 66-year-old woman. **(A)** Sagittal FDG PET (left) and fused FDG PET/CT (middle) images show mild FDG uptake throughout the bone marrow, only slightly above that of blood pool, which could be marrow disease or reactive marrow. Sagittal CT image (right) shows subtle but diffuse lytic and sclerotic changes suggestive of metastasis (SUV scale, 0–4.6). **(B)** Sagittal FES PET (left) and fused FES PET/CT (right) images show clearly abnormal FES uptake in the bones, which is highly suspicious for functionally ER-positive metastasis (SUV scale, 0–3). Years of clinical and imaging follow-up demonstrated widespread sclerotic osseous metastasis.

Studies have also been performed to investigate the use of FES to predict patient response to ER-targeted therapy (Figs 21, 22). In fact, in a 2006 study, Linden et al (48) showed that none of the 15 patients (0%) with ER-positive breast cancer according to immunohistochemical results and FES-negative disease responded to ER-targeted therapy. This study

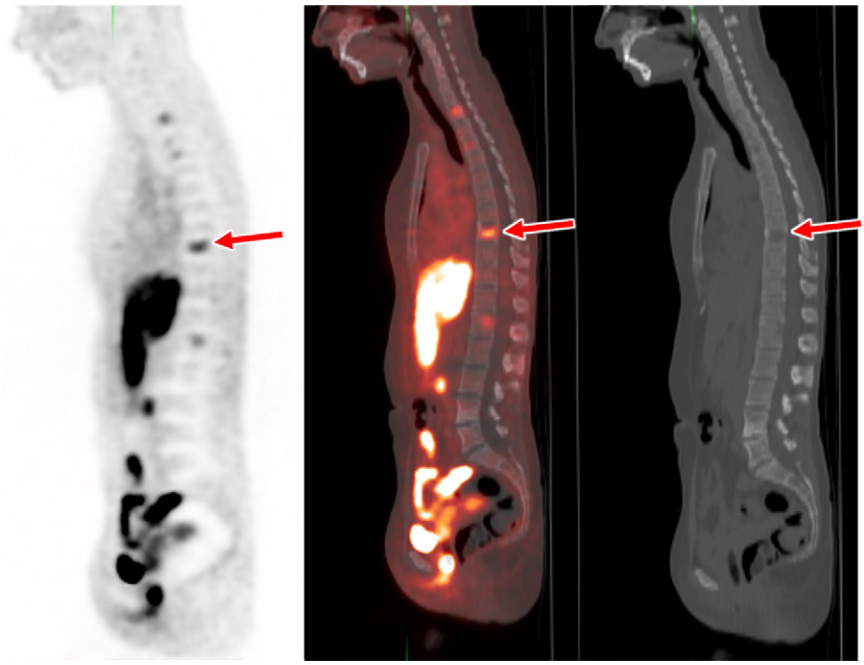

Figure 16. Metastatic ER-positive poorly differentiated invasive ductal carcinoma in a 35-year-old woman. Sagittal FES PET (left) and sagittal fused FES PET/CT (middle) images show abnormal FES uptake (arrows, left and middle) in multiple vertebrae, which are easily identified among the non–FES-avid normal vertebrae. Sagittal CT image (right) shows lucent lesions (arrow, right) corresponding to the abnormal FES uptake. FES uptake in osseous structures is easily characterized as metastasis even without a corresponding CT abnormality, because degenerative osseous disease does not demonstrate FES avidity. Although bone biopsy was not performed, the patient had years of clinical and imaging follow-up that demonstrated ER-positive osseous metastatic disease (SUV scale, 0–5).

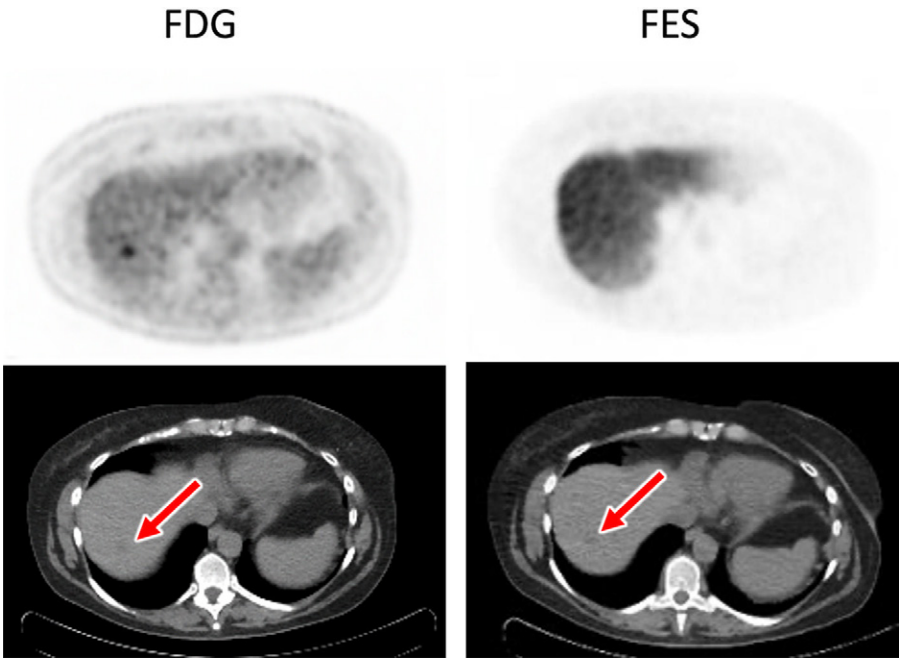

Figure 17. ER-positive, PR-positive, ERBB2-negative poorly differentiated invasive ductal carcinoma in a 62-year-old woman. Axial FDG PET (top left) and CT (bottom left) images show an FDG-avid liver dome metastasis as a small area of hypoattenuation (arrow, bottom left) (SUV scale, 0–5). ER-positive hepatic metastasis was confirmed at subsequent biopsy. Axial FES PET image (top right) acquired 15 days earlier shows diffuse homogeneous background FES uptake in the liver, without a discrete liver metastasis (SUV scale, 0–15). Corresponding axial CT image (bottom right) shows a subtle hypoattenuating lesion (arrow, bottom right). The small ER-positive hepatic lesion is likely not identified on FES images because of the high background FES liver uptake.

highlights the high predictive value of a negative FES scan and emphasizes that FES likely allows imaging of functional ER expression, which may not be adequately evaluated at immunohistochemical analysis but may be important clinically. In addition, in this study, 23% of patients responded to ER-targeted therapy, but this number increased to 34% when patients were confirmed to have FES-positive disease, again suggesting a clinically important functional ER assessment with the use of FES (48).

In a 2013 article, van Kruchten et al (49) performed a pooled analysis of four studies in which the use of FES to predict the response to ER-targeted therapy was evaluated and found that 37 of 42 (88%) patients with tumor FES uptake of less than 1.5 who underwent endocrine therapy experienced treatment failure, resulting in a negative predictive value for FES PET/CT of 88%. This same pooled analysis showed that a positive FES scan can help to identify patients who will demonstrate a clinical response to endocrine therapy, with a positive predictive value of 65% (49). Investigators have also harnessed FES homogeneity to predict outcomes, showing that patients with heterogeneous FES uptake have worse outcomes than those with homogeneously FES-positive disease (45). Future research is needed to optimize treatment of ER-positive/FES-negative patients and ER-heterogeneous patients, with FES PET/CT as a possibly crucial imaging study in these populations.

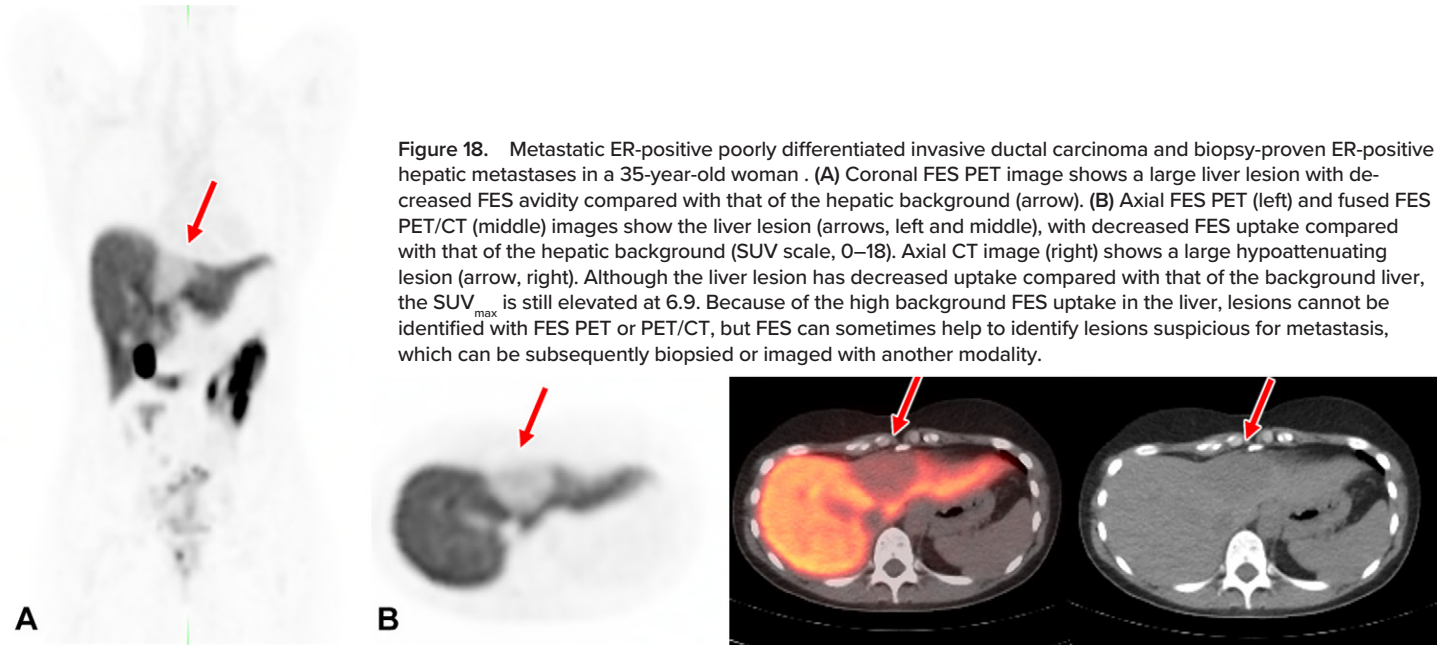

Figure 18. Metastatic ER-positive poorly differentiated invasive ductal carcinoma and biopsy-proven ER-positive hepatic metastases in a 35-year-old woman . **(A)** Coronal FES PET image shows a large liver lesion with decreased FES avidity compared with that of the hepatic background (arrow). **(B)** Axial FES PET (left) and fused FES PET/CT (middle) images show the liver lesion (arrows, left and middle), with decreased FES uptake compared with that of the hepatic background (SUV scale, 0–18). Axial CT image (right) shows a large hypoattenuating lesion (arrow, right). Although the liver lesion has decreased uptake compared with that of the background liver, the SUV_{max} is still elevated at 6.9. Because of the high background FES uptake in the liver, lesions cannot be identified with FES PET or PET/CT, but FES can sometimes help to identify lesions suspicious for metastasis, which can be subsequently biopsied or imaged with another modality.

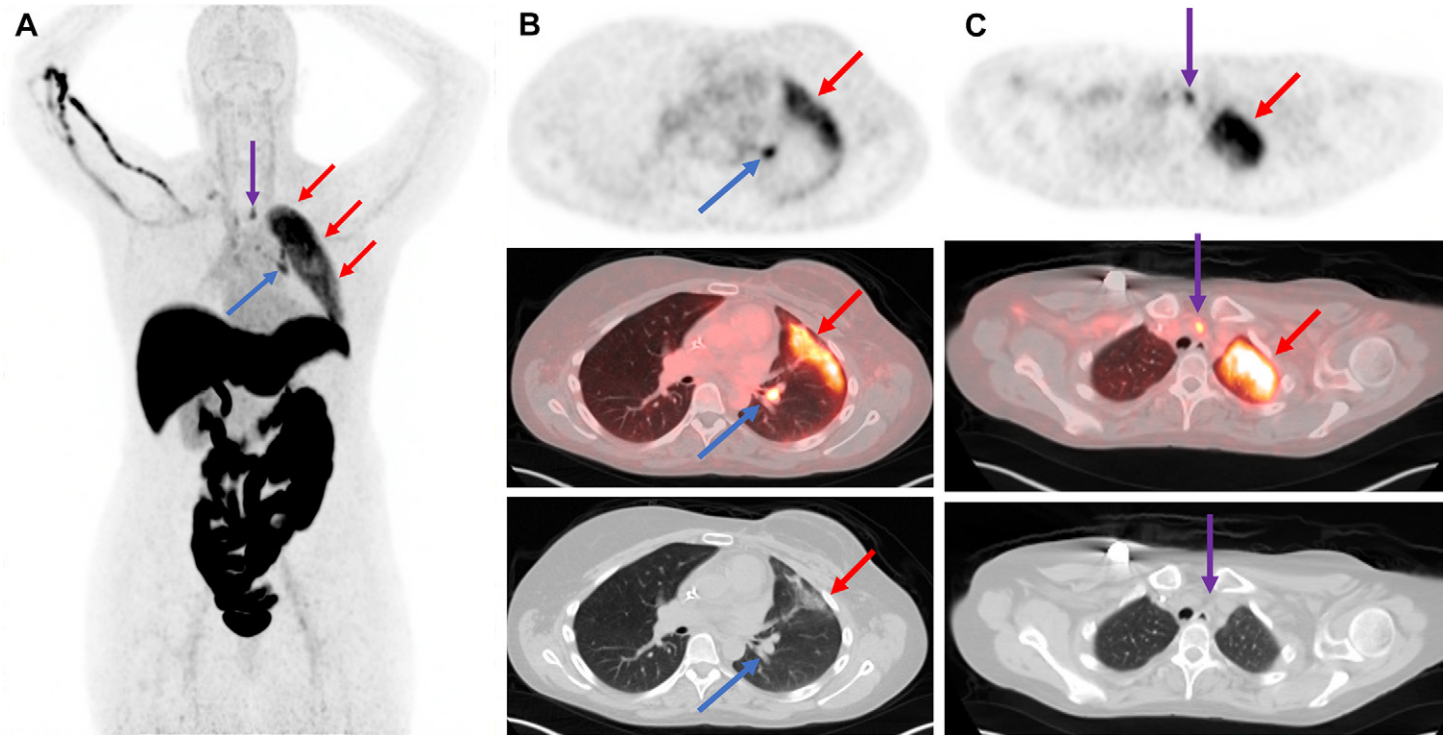

Figure 19. ER-positive, PR-negative, ERBB2-positive metastatic invasive ductal carcinoma in a 34-year-old woman who underwent sternal radiation therapy. **(A)** Coronal MIP FES PET image shows abnormal FES uptake in the left lung (red arrows), the supraclavicular lymph node (purple arrow), and a left hilar node (blue arrow). **(B)** Axial FES PET (top) and fused FES PET/CT (middle) images also show abnormal FES uptake in the anterior left lung (red arrows, top and middle) and left hilar node (blue arrows, top and middle), with axial CT image (bottom) showing the anatomic correlates in the left lung (red arrow, bottom) and left hilar node (blue arrow, bottom). The FES uptake in the left lung correlates with peripheral ground-glass opacities suggestive of radiation pneumonitis, a false-positive finding. **(C)** Axial FES PET (top) and fused FES PET/CT (middle) images show abnormal FES uptake in the left lung (red arrows) and the supraclavicular lymph node (purple arrows, top and middle). Axial anatomic CT image (bottom) localizes the left supraclavicular lymph node (purple arrow, bottom) (SUV scale, 0–5).

Authors of other studies have used FES to demonstrate effective ER blockade with ER-antagonist therapy (Fig 23). Patients with incomplete ER blockade at FES PET/CT have been shown to have earlier disease progression than those with complete ER blockade (19). After this discovery, FES PET was used to determine the dose of an ER-antagonist needed for complete ER blockade (20). Determining the dose on the basis of imaging evidence of blockade of a metabolic target is a specific application of a radiotracer that differs from the typical use of radiotracers in clinical diagnostic imaging.

Figure 20. ER-positive poorly differentiated grade 3 ductal carcinoma of the left breast, with widespread osseous metastasis, in a 70-year-old woman. The patient underwent screening colonoscopy with biopsy of a cecal lesion revealing ER-positive metastasis. Axial FES PET (left), anatomic CT (middle), and fused FES PET/CT (right) images show abnormal FES avidity of the ER-positive cecal mass (red arrows) and lumbar vertebra (blue arrow, left) and non-FES-avid loops of the distal large bowel (green arrows, right) (SUV scale, 0–5). Efficient resorption of FES metabolites leads to high FES background activity of the small bowel and minimal to no FES uptake in the large bowel. Careful adjustment of windows is required for evaluation of the bowel.

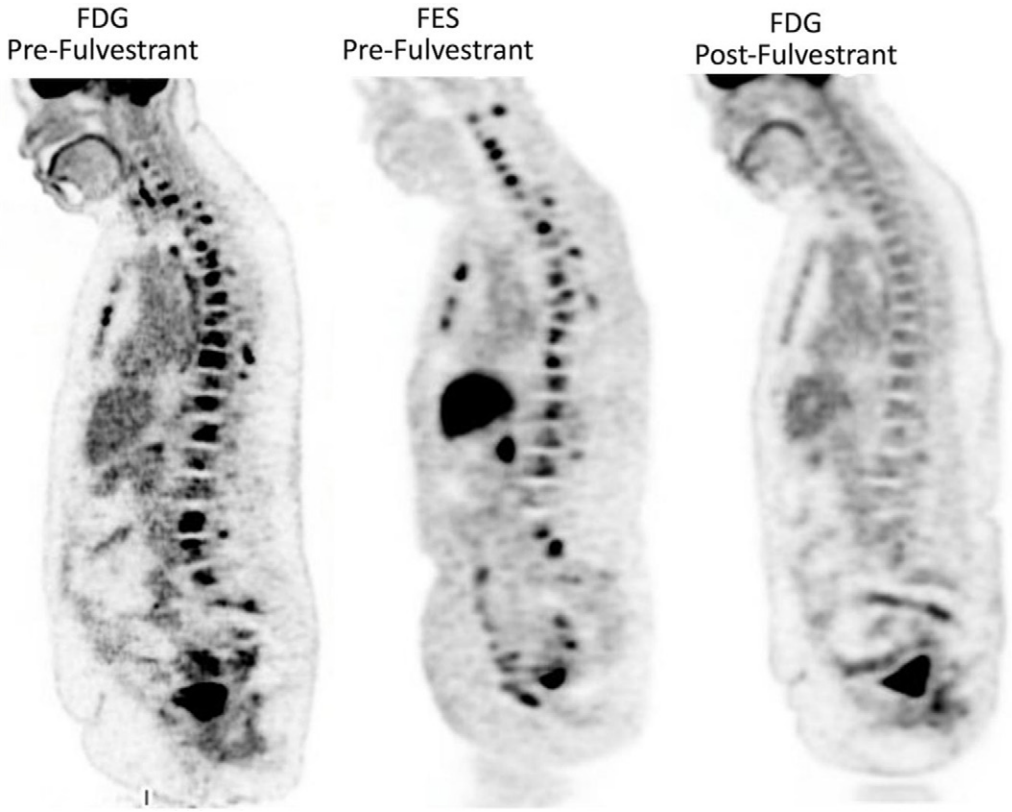

Figure 21. Biopsy-proven metastatic ER-positive, PR-positive, ERBB2-negative adenocarcinoma most likely of mammary origin in a 72-year-old woman. Sagittal FDG PET image (left) shows widely metastatic osseous FDG-avid disease, and sagittal FES PET image (middle) shows concordant FES-positive osseous disease. The patient began ER-targeted therapy with fulvestrant. Subsequently acquired FDG PET image (right) shows complete metabolic response to therapy. Patients with FDG-avid disease before ER-targeted therapy can undergo follow-up FDG PET, because the use of FES is severely limited in those undergoing ER-antagonist therapy (SUV scale, 0–5).

This method of dose determination is also different from that used in typical dose-escalation trials, in which dosing is determined on the basis of observed toxicity.

In addition, FES PET/CT is being investigated for use in other malignancies that express ER, most notably uterine and endometrial cancer and less so in ovarian cancers, although clear demonstration of utility has not been found, to our knowledge (50–53). Although there is some preliminary evidence that abnormal FES uptake may allow prediction of prognosis in patients with endometrial cancer, there are no data to guide whether uterine uptake is physiologic or malignant (54). High normal uterine uptake of FES limits interpretation of FES in this patient population, and more research is needed to determine its clinical utility. To our knowledge, there are few reports of the use of FES PET in patients with ovarian cancer. One limitation to the use of FES in patients with ovarian cancer is that cystic components of ovarian malignancy are common but are negative for FES uptake. However, results of a small study (53) demonstrated a correlation between abnormal FES uptake in ovarian tumors and metastases with subsequent histologic evaluation performed at debulking surgery. More research is needed in this area.

Conclusion

FES is a PET radiotracer that targets the ER and was recently approved for use in patients with metastatic ER-positive breast cancer in France and the United States. As an in vivo measure of ER expression and ER-binding function, FES is an example of precision medicine that has been leveraged to optimize the care of patients with breast cancer. As clinical and research

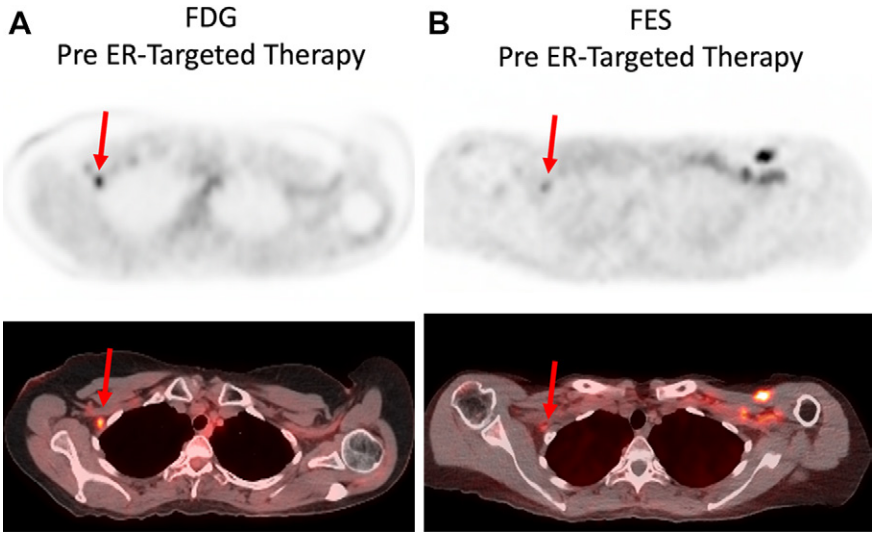

Figure 22. ER-positive bilateral invasive ductal carcinoma in a 66-year-old patient who underwent bilateral lumpectomy and radiation. **(A)** Axial restaging FDG PET (top) and fused FDG PET/CT (bottom) images show abnormal FDG uptake in a right axillary lymph node (arrows) that is suspicious for recurrent disease (SUV_{max}, 3.8). **(B)** Axial FES PET (top) and fused FES PET/CT (bottom) images show concordant abnormal FES avidity in the right axillary lymph node (arrows) that is suggestive of functionally ER-positive metastasis (SUV_{max}, 2.1; SUV scale, 0–5). Abnormal FES uptake was also seen in the liver and bones (not shown), corresponding to the abnormal uptake seen on FDG images. Subsequent right axillary excision allowed confirmation of ER-positive metastasis. The FES uptake in the left anterior chest is residual tracer in collateral vessels from left-sided FES administration. Subsequent FDG PET/CT images (not shown) showed a complete metabolic response after initiation of ER-targeted therapy with fulvestrant and a CDK4 or CDK6 inhibitor. Patients who show FDG avidity before ER-targeted therapy can be followed up with FDG PET, because FES imaging in patients undergoing ER-antagonist therapy is severely limited.

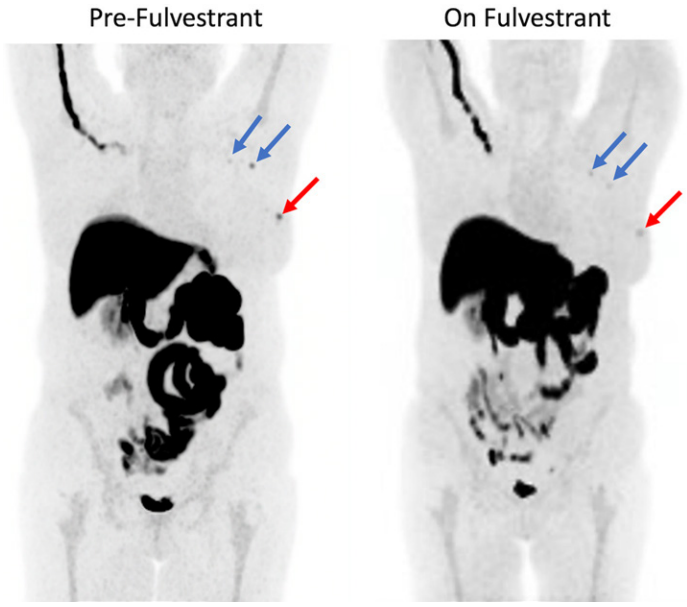

Figure 23. ER-positive, PR-positive, ERBB2-negative bilateral invasive ductal carcinoma with osseous metastases in a 60-year-old woman who was previously in remission and presented with a new biopsy-proven ER-positive invasive ductal carcinoma on the left side. Coronal MIP FES PET image (left) shows FES-positive breast cancer (red arrow, left; SUV_{max}, 3.3) and previously unknown FES-positive left axillary lymph nodes suggestive of nodal metastases (blue arrows, left; SUV_{max}, 3.1). Coronal MIP FES PET image (right) acquired after 3 months of ER-antagonist therapy with fulvestrant shows decreased but residual FES uptake in the left breast cancer (red arrow, right; SUV_{max}, 2.1) and left axillary nodal metastases (blue arrows, right; SUV_{max}, 1.8) suggestive of incomplete ER blockade (SUV scale, 0–5 for all images).

experience with this tracer grows, we expect even further benefits, with increased indications in patients with breast cancer including its use as a predictive biomarker for targeted therapy.

Author affiliations.—From the Department of Radiology, Division of Breast Imaging (S.R.O., C.E.E.) and Division of Nuclear Medicine Imaging and Therapy (S.R.O., S.M.L., J.K.W., D.A.M., A.R.P.), Hospital of the University of Pennsylvania, 3400 Spruce St, 1 Silverstein–Radiology Administration, Philadelphia, PA 19104. Presented as an education exhibit at the 2021 RSNA Annual Meeting. Received June 8, 2022; revision requested July 14 and received August 7; accepted August 9. **Address correspondence to** S.R.O. (email: *Sophia.Obrien@pennmedicine.upenn.edu*).

Disclosures of conflicts of interest.—**S.R.O.** Honoraria for lectures from the Society of Nuclear Medicine and Molecular Imaging (SNMMI), support for travel from GE. **D.A.M.** Payments for consultancy from GE. **A.R.P.** Institutional support from Lantheus; consultancy for Blue Earth Diagnostics, Progenics, and GE.; honoraria and travel support from the SNMMI.

References

1. National Cancer Institute. Cancer Stat Facts: Female Breast Cancer Subtypes. Surveillance, Epidemiology, and End Results Program. https://seer.cancer.gov/statfacts/html/breast-subtypes.html. Published 2021. Accessed July 27, 2022.
2. World Cancer Research Fund International. Breast Cancer Statistics 2021. https://www.wcrf.org/cancer-trends/breast-cancer-statistics/. Accessed November 28, 2022.
3. U.S. Cancer Statistics Working Group. U.S. Cancer Statistics Data Visualizations Tool, based on 2020 submission data (1999–2018). U.S. Department of Health and Human Services, Centers for Disease Control and Prevention and National Cancer Institute. https://www.cdc.gov/cancer/dataviz. Updated October 20, 2022. Accessed November 28, 2022.
4. American Cancer Society. Cancer Facts & Figures for African American/Black People 2022–2024. https://www.cancer.org/research/cancer-facts-statistics/cancer-facts-figures-for-african-americans.html. Published February 14, 2022. Accessed November 28, 2022.
5. National Comprehensive Cancer Network. NCCN Clinical Practice Guidelines in Oncology: Breast Cancer. Version 3.2022. Plymouth Meeting, Pa: National Comprehensive Cancer Network, 2022.
6. Zeng J, Piscuoglio S, Aggarwal G, et al. Hormone receptor and HER2 assessment in breast carcinoma metastatic to bone: A comparison between FNA cell blocks and decalcified core needle biopsies. Cancer Cytopathol 2020;128(2):133–145.
7. Aurilio G, Monfardini L, Rizzo S, et al. Discordant hormone receptor and human epidermal growth factor receptor 2 status in bone metastases compared to primary breast cancer. Acta Oncol 2013;52(8):1649–1656.
8. Fluoroestradiol (18F) ESTROTEP 500 MBq/mL solution for injection Re-evaluation. https://www.has-sante.fr/upload/docs/application/pdf/2020-05/estrotep_summary_ct18010.pdf. February 18, 2020.
9. U.S. Food and Drug Administration. Cerianna (Fluoroestradiol F18). Full Prescribing Information. https://www.accessdata.fda.gov/drugsatfda_docs/label/2020/212155s000lbl.pdf. Updated May 2020.
10. Katzenellenbogen JA. The quest for improving the management of breast cancer by functional imaging: The discovery and development of 16α-[^{18}F]fluoroestradiol (FES), a PET radiotracer for the estrogen receptor, a historical review. Nucl Med Biol 2021;92:24–37.
11. Mintun MA, Welch MJ, Siegel BA, et al. Breast cancer: PET imaging of estrogen receptors. Radiology 1988;169(1):45–48.
12. Peterson LM, Mankoff DA, Lawton T, et al. Quantitative imaging of estrogen receptor expression in breast cancer with PET and 18F-fluoroestradiol. J Nucl Med 2008;49(3):367–374.

13. Chae SY, Ahn SH, Kim SB, et al. Diagnostic accuracy and safety of 16α-[^{18}F] fluoro-17β-oestradiol PET-CT for the assessment of oestrogen receptor status in recurrent or metastatic lesions in patients with breast cancer: a prospective cohort study. Lancet Oncol 2019;20(4):546–555.
14. Mankoff DA, Peterson LM, Tewson TJ, et al. [18F]fluoroestradiol radiation dosimetry in human PET studies. J Nucl Med 2001;42(4):679–684.
15. Mankoff DA, Tewson TJ, Eary JF. Analysis of blood clearance and labeled metabolites for the estrogen receptor tracer [F-18]-16 alpha-fluoroestradiol (FES). Nucl Med Biol 1997;24(4):341–348.
16. Sundararajan L, Linden HM, Link JM, Krohn KA, Mankoff DA. 18F-Fluoroestradiol. Semin Nucl Med 2007;37(6):470–476.
17. Peterson LM, Kurland BF, Schubert EK, et al. A phase 2 study of 16α-[18F]-fluoro-17β-estradiol positron emission tomography (FES-PET) as a marker of hormone sensitivity in metastatic breast cancer (MBC). Mol Imaging Biol 2014;16(3):431–440 [Published correction appears in Mol Imaging Biol 2019;21(1):191.].
18. Mo JA. Safety and Effectiveness of F-18 Fluoroestradiol Positron Emission Tomography/Computed Tomography: a Systematic Review and Meta-analysis. J Korean Med Sci 2021;36(42):e271.
19. van Kruchten M, de Vries EG, Glaudemans AW, et al. Measuring residual estrogen receptor availability during fulvestrant therapy in patients with metastatic breast cancer. Cancer Discov 2015;5(1):72–81.
20. Wang Y, Ayres KL, Goldman DA, et al. ^{18}F-Fluoroestradiol PET/CT Measurement of Estrogen Receptor Suppression during a Phase I Trial of the Novel Estrogen Receptor-Targeted Therapeutic GDC-0810: Using an Imaging Biomarker to Guide Drug Dosage in Subsequent Trials. Clin Cancer Res 2017;23(12):3053–3060 [Published correction appears in Clin Cancer Res 2019;25(4):1435.].
21. Goel S, DeCristo MJ, McAllister SS, Zhao JJ. CDK4/6 Inhibition in Cancer: Beyond Cell Cycle Arrest. Trends Cell Biol 2018;28(11):911–925.
22. Peterson LM, Kurland BF, Link JM, et al. Factors influencing the uptake of 18F-fluoroestradiol in patients with estrogen receptor positive breast cancer. Nucl Med Biol 2011;38(7):969–978.
23. Jamar F, Buscombe J, Chiti A, et al. EANM/SNMMI guideline for 18F-FDG use in inflammation and infection. J Nucl Med 2013;54(4):647–658.
24. Dilsizian V, Metter D, Palestro C, Zanzonico P. Advisory Committee on Medical Uses of Isotopes (ACMUI) Sub-Committee on Nursing Mother Guidelines for the Medical Administration of Radioactive Materials. https://www.nrc.gov/docs/ML1803/ML18033B034.pdf. February 1, 2018.
25. Liao GJ, Clark AS, Schubert EK, Mankoff DA. 18F-Fluoroestradiol PET: Current Status and Potential Future Clinical Applications. J Nucl Med 2016;57(8):1269–1275.
26. Kurland BF, Wiggins JR, Coche A, et al. Whole-Body Characterization of Estrogen Receptor Status in Metastatic Breast Cancer with 16α-18F-Fluoro-17β-Estradiol Positron Emission Tomography: Meta-Analysis and Recommendations for Integration into Clinical Applications. Oncologist 2020;25(10):835–844.
27. Chae SY, Son HJ, Lee DY, et al. Comparison of diagnostic sensitivity of [^{18}F] fluoroestradiol and [^{18}F]fluorodeoxyglucose positron emission tomography/computed tomography for breast cancer recurrence in patients with a history of estrogen receptor-positive primary breast cancer. EJNMMI Res 2020;10(1):54.
28. Evangelista L, Guarneri V, Conte PF. 18F-Fluoroestradiol Positron Emission Tomography in Breast Cancer Patients: Systematic Review of the Literature & Meta-Analysis. Curr Radiopharm 2016;9(3):244–257.
29. van Geel JJL, Boers J, Elias SG, et al. Clinical Validity of 16α-[^{18}F]Fluoro-17β-Estradiol Positron Emission Tomography/Computed Tomography to Assess Estrogen Receptor Status in Newly Diagnosed Metastatic Breast Cancer. J Clin Oncol 2022. 10.1200/JCO.22.00400. Published online May 18, 2022. Accessed November 28, 2022.
30. Patanaphan V, Salazar OM, Risco R. Breast cancer: metastatic patterns and their prognosis. South Med J 1988;81(9):1109–1112.
31. Mollerup S, Jørgensen K, Berge G, Haugen A. Expression of estrogen receptors alpha and beta in human lung tissue and cell lines. Lung Cancer 2002;37(2):153–159.
32. Dieci MV, Barbieri E, Piacentini F, et al. Discordance in receptor status between primary and recurrent breast cancer has a prognostic impact: a single-institution analysis. Ann Oncol 2013;24(1):101–108.
33. Kurland BF, Peterson LM, Lee JH, et al. Estrogen Receptor Binding (18F-FES PET) and Glycolytic Activity (18F-FDG PET) Predict Progression-Free Survival on Endocrine Therapy in Patients with ER+ Breast Cancer. Clin Cancer Res 2017;23(2):407–415.
34. Hoefnagel LD, van de Vijver MJ, van Slooten HJ, et al. Receptor conversion in distant breast cancer metastases. Breast Cancer Res 2010;12(5):R75.
35. van Kruchten M, Glaudemans AW, de Vries EF, et al. PET imaging of estrogen receptors as a diagnostic tool for breast cancer patients presenting with a clinical dilemma. J Nucl Med 2012;53(2):182–190.
36. Sari E, Guler G, Hayran M, Gullu I, Altundag K, Ozisik Y. Comparative study of the immunohistochemical detection of hormone receptor status and HER-2 expression in primary and paired recurrent/metastatic lesions of patients with breast cancer. Med Oncol 2011;28(1):57–63.
37. van de Ven S, Smit VT, Dekker TJ, Nortier JW, Kroep JR. Discordances in ER, PR and HER2 receptors after neoadjuvant chemotherapy in breast cancer. Cancer Treat Rev 2011;37(6):422–430.
38. Currin E, Peterson LM, Schubert EK, et al. Temporal Heterogeneity of Estrogen Receptor Expression in Bone-Dominant Breast Cancer: 18F-Fluoroestradiol PET Imaging Shows Return of ER Expression. J Natl Compr Canc Netw 2016;14(2):144–147.
39. Kurland BF, Peterson LM, Lee JH, et al. Between-patient and within-patient (site-to-site) variability in estrogen receptor binding, measured in vivo by 18F-fluoroestradiol PET. J Nucl Med 2011;52(10):1541–1549.
40. Boers J, Loudini N, de Haas RJ, et al. Analyzing the Estrogen Receptor Status of Liver Metastases with [^{18}F]-FES-PET in Patients with Breast Cancer. Diagnostics (Basel) 2021;11(11):2019.
41. Telugu RB, Chowhan AK, Rukmangadha N, et al. Estrogen and progesterone receptor in meningiomas: An immunohistochemical analysis. J Cancer Res Ther 2020;16(6):1482–1487.
42. Borahay MA, Asoglu MR, Mas A, Adam S, Kilic GS, Al-Hendy A. Estrogen Receptors and Signaling in Fibroids: Role in Pathobiology and Therapeutic Implications. Reprod Sci 2017;24(9):1235–1244.
43. Venema CM, de Vries EFJ, van der Veen SJ, et al. Enhanced pulmonary uptake on ^{18}F-FES-PET/CT scans after irradiation of the thoracic area: related to fibrosis? EJNMMI Res 2019;9(1):82.
44. O'Brien SR, Edmonds CE, Katz D, Mankoff DA, Pantel AR. 18F-Fluoroestradiol (FES) PET/CT: review of current practice and future directions. Clin Transl Imaging 2022;10(4):331–341.
45. Boers J, Venema CM, de Vries EFJ, et al. Molecular imaging to identify patients with metastatic breast cancer who benefit from endocrine treatment combined with cyclin-dependent kinase inhibition. Eur J Cancer 2020;126:11–20.
46. Venema C, de Vries E, Glaudemans A, Poppema B, Hospers G, Schröder C. 18F-FES PET Has Added Value in Staging and Therapy Decision Making in Patients With Disseminated Lobular Breast Cancer. Clin Nucl Med 2017;42(8):612–614.
47. Ulaner GA, Jhaveri K, Chandarlapaty S, et al. Head-to-Head Evaluation of ^{18}F-FES and ^{18}F-FDG PET/CT in Metastatic Invasive Lobular Breast Cancer. J Nucl Med 2021;62(3):326–331.
48. Linden HM, Stekhova SA, Link JM, et al. Quantitative fluoroestradiol positron emission tomography imaging predicts response to endocrine treatment in breast cancer. J Clin Oncol 2006;24(18):2793–2799.
49. van Kruchten M, de Vries EGE, Brown M, et al. PET imaging of oestrogen receptors in patients with breast cancer. Lancet Oncol 2013;14(11):e465–e475.
50. Tsujikawa T, Yoshida Y, Kiyono Y, et al. Functional oestrogen receptor α imaging in endometrial carcinoma using 16α-[^{18}F]fluoro-17β-oestradiol PET. Eur J Nucl Med Mol Imaging 2011;38(1):37–45.
51. Yoshida Y, Kiyono Y, Tsujikawa T, Kurokawa T, Okazawa H, Kotsuji F. Additional value of 16α-[18F]fluoro-17β-oestradiol PET for differential diagnosis between uterine sarcoma and leiomyoma in patients with positive or equivocal findings on [18F]fluorodeoxyglucose PET. Eur J Nucl Med Mol Imaging 2011;38(10):1824–1831.
52. Yoshida Y, Kurokawa T, Tsujikawa T, Okazawa H, Kotsuji F. Positron emission tomography in ovarian cancer: 18F-deoxy-glucose and 16alpha-18F-fluoro-17beta-estradiol PET. J Ovarian Res 2009;2(1):7.
53. van Kruchten M, de Vries EF, Arts HJ, et al. Assessment of estrogen receptor expression in epithelial ovarian cancer patients using 16α-18F-fluoro-17β-estradiol PET/CT. J Nucl Med 2015;56(1):50–55.
54. Yamada S, Tsuyoshi H, Yamamoto M, et al. Prognostic Value of 16α-^{18}F-Fluoro-17β-Estradiol PET as a Predictor of Disease Outcome in Endometrial Cancer: A Prospective Study. J Nucl Med 2021;62(5):636–642.